Title
OPTICAL ABSORPTION SPECTRA OF MATRIX-ISOLATED COPPER, SILVER AND GOLD

Author
King, Baldwin A.

Publication Date
1968-11-01

UCRL-18618

cy. 2

OPTICAL ABSORPTION SPECTRA OF MATRIX-ISOLATED COPPER, SILVER AND GOLD

Baldwin A. King
(Ph.D. Thesis)

November 1968

UCRL-18618

cy. 2

LAWRENCE RADIATION LABORATORY
UNIVERSITY of CALIFORNIA BERKELEY

DISCLAIMER

UCRL-18618

UNIVERSITY OF CALIFORNIA

Lawrence Radiation Laboratory
Berkeley, California
AEC Contract No. W-7405-eng-48

OPTICAL ABSORPTION SPECTRA OF MATRIX-ISOLATED COPPER, SILVER AND GOLD

Baldwin A. King

(Ph.D. Thesis)

November 1968

TABLE OF CONTENTS

OPTICAL ABSORPTION SPECTRA OF MATRIX-ISOLATED COPPER, SILVER AND GOLD

Baldwin A. King

Inorganic Materials Research Division, Lawrence Radiation Laboratory,
and Department of Chemistry,
University of California, Berkeley, California

ABSTRACT

Copper atoms are trapped at 20 Kelvin in krypton and xenon, silver atoms in argon, krypton and xenon, gold atoms in krypton, xenon and sulfur hexafluoride. The transitions $np\ ^2P \leftarrow ns\ ^2S$ are studied in absorption and are found to be blue shifted from the free atom positions except for gold in xenon. Three strong bands are observed in all cases except for gold in sulfur hexafluoride which gives two bands. Absorption spectra are also recorded for silver co-condensed with sulfur hexafluoride and n-perfluoroheptane, copper with sulfur hexafluoride and gold with n-perfluoroheptane.

I. INTRODUCTION

The generation and trapping of high temperature molecules in solid matrices is of interest for a number of reasons. For example the vapor phase spectra of these molecules may be complex and difficult to resolve. This occurs partly because the Boltzmann population of states other than the ground vibronic state is not negligible at these high temperatures and absorption spectra often consist of many overlapping progressions. However at very low temperatures the molecules, trapped in a solid medium are expected to be found only in the $v'' = 0$ level of the ground electronic state. Then only transitions involving states connected to the ground state occur in absorption and in principle this should make the analysis of the spectra of the species a less complicated matter. It may be that the ground state of the gaseous molecule is in doubt as in the case of ScF. Then if complications due to the solvent are absent, it should be possible to decide among the different alternatives by trapping the species in the solvent at low temperatures. Unfortunately the situation is not so straight forward because the solute often experiences perturbations of its energy levels coincident with the presence of neighboring solvent molecules. These matrix effects may include broadening of lines and shifts of their maxima from free atom positions and the appearance of multiplet structures.

Occasionally the electronic transition probabilities of the solute seem to be affected to some extent. For example the highly forbidden $^2D_{5/2,3/2} \leftarrow {}^4S_{3/2}$ transitions in the free N atom have a half life of about 20 hours. In a solid matrix the strongest transition is believed to

be of the order of 10-20 seconds.* Frosch† found the lifetime of the

*Herzfeld C.: Phys. Rev. 107 1239 (1957).

†Frosch, R.: Ph.D. Thesis, 1965 Univ. Microfilm, Ann Arbor, Michigan.

excited state of the M-bands of NO trapped in Ne, Ar, Kr to be dependent on the matrix type (156, 93 and 35 msec respectively) and probably different from the gas phase. These effects are interesting in themselves and their understanding may add to our knowledge of the broader topic of molecular interactions in the solid state. It would seem appropriate then to select some solute and see what effect the solvent has on its optical spectra as we go through the range of nonpolar to polar solvents. Atoms would be the choice as solutes because their spectra are inherently simpler than molecules. If we obtained a fair understanding of the detailed behavior of a given atomic species as we go from one solid environment to another we could then try to predict with reasonable confidence the probable behavior of other atoms and eventually molecules.

This thesis reports the results of a study of the optical absorption spectra of copper, silver and gold in a number of matrices.

II. THEORY AND LITERATURE SURVEY

A. Line Shifts in Matrix Spectra

Studies of the perturbation of atomic lines due to the presence of foreign gases have been going on since the 1890's and the behavior of atoms in these high density gases may be looked upon as the precursor of that in the solid matrix. In particular, shifts and broadening of the lines are already apparent. For example Ch'en et al.* studied the effect of

*Ch'en S. Y., Bennett R. B., Jetimenko O.: JOSA 46, 182 (1956).

krypton and xenon at a pressure of one atmosphere on the absorption doublets belonging to the principal series ($np\ ^2P \leftarrow 5s\ ^2S$) of the rubidium atom. Satellite bands were seen both to the red and blue of the atomic doublets, the blue bands appearing only at relatively high vapor pressures of Rb.

An impurity atom frozen into a solid matrix experiences even larger perturbations of its energy levels by the matrix molecules. Because the ground and excited states of the solute are affected to a different extent, spectral shifts result which may be either to the red or to the blue of the free atom positions. Red shifts are apparently due to long-range attractive dispersion interactions of an induced dipole-induced dipole nature. Physically there seems to be a delocalization of the electrons of the solute and solvent into the intermolecular band. Effectively the emission electron is then less firmly bound to the atom and consequently has its excitation energy lowered. One expression due to Longuet-Higgins

and Pople relates the polarisabilities to the red shift ΔE as follows

$$\Delta E = \frac{3}{8} \alpha_v \alpha_n z r_{nv}^{-6} E_n$$

where α_v, α_n are the molecular polarisabilities of the solvent and solute respectively, z is the density of nearest-neighbor solvent molecules, r_{nv} the mean intermolecular distance and E_n the energy of transition of the solute. Calculations based on this equation give the right order of magnitude for the shifts.

Blue shifts seem to originate from short-range repulsive exchange interactions in systems where large solute molecules are embedded in a lattice of small solvent molecules. The excitation of the valence electron of the solute out of the ground state and into Rydberg orbitals, results in an extension of the electron cloud. The Pauli Exclusion Principle however prevents any appreciable overlap of the Rydberg orbitals of the electron of the solute with the filled orbitals of the solvent molecule. The net effect is that the energy of the valence electron in its excited state is raised relative to the ground state, thus causing a blue shift of the transition energy.

It has been observed in the study of matrix-isolated atoms that blue shifts decrease in the order argon, krypton, xenon which is also the order of increasing polarisability and increasing lattice parameter.

B. Multiplet Splitting Effects in Matrix Spectra

1. F-Center Analogy.

A pure, transparent single crystal of alkali halide becomes deeply colored on being heated in the presence of alkali metal vapor. The absorp-

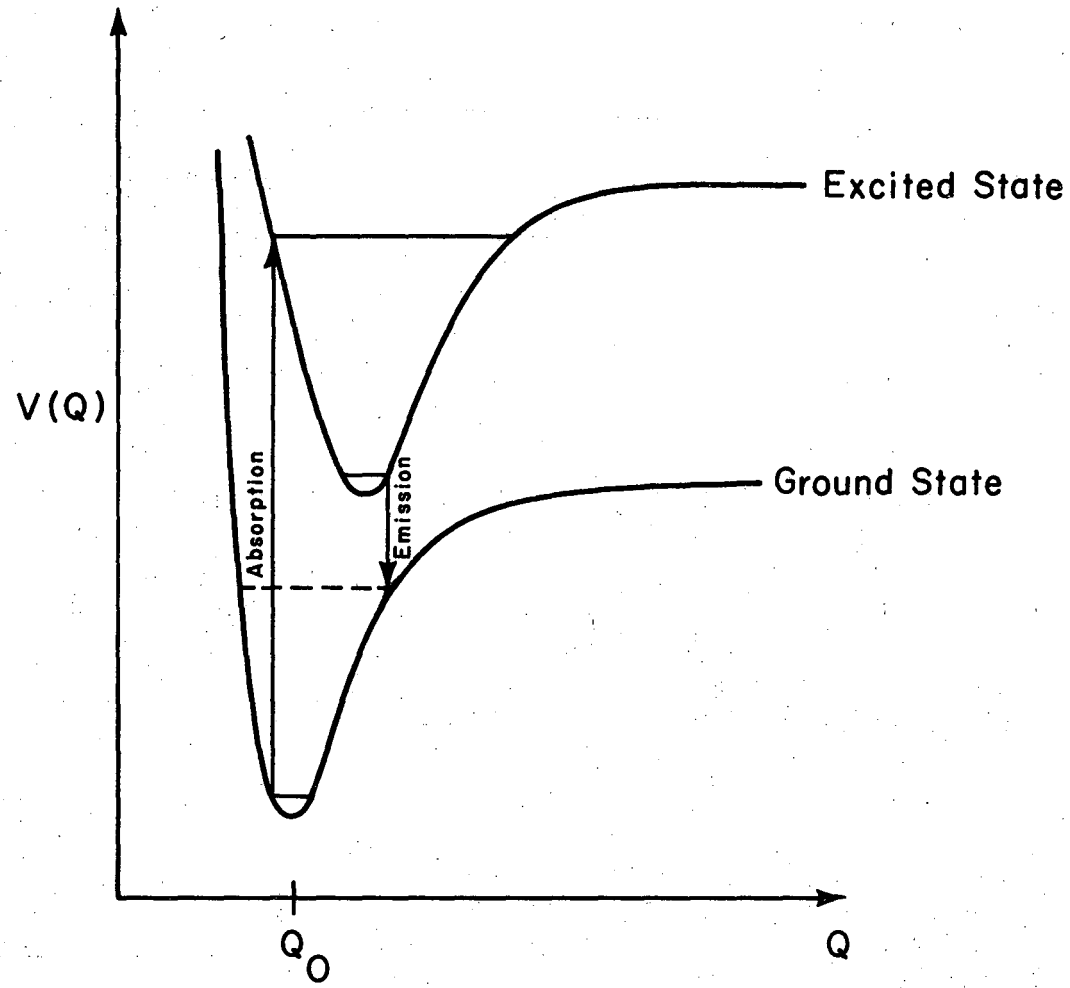

XBL 6810-6065

Fig. 1 Configuration coordinate diagram for localized F-center

tion spectrum of treated KCl, cooled to 90 K, exhibits a broad band with peak intensity at 539.0 nm and a half-width of 1600 cm^{-1}. The occurrence and properties of this F-band have been successfully explained on the assumption that the F-center is an electron trapped at an anion vacancy in the crystal lattice.* The absorption maximum of the F-band is observed to

---

*Schulman J.H., Compton W.B.:Color Centers in Solids. Pergamon 1962.

---

be strongly temperature dependent and to bear a fairly simple relationship to the interionic distance . The interaction of the trapped electron with the neighboring ions has been studied extensively by ESR which among other things establishes the high symmetry of the F-center.

The theoretical treatment of the F-center problem consists essentially of the evaluation of the potential the trapped electron sees under the influence of the lattice ions. Some approximations take account only of the short-range interactions between F-center and its nearest-neighbor alkali ions, while others consider long-range interactions with the lattice vibrations. Attempts are then made to calculate the wavefunctions and energy levels of the electron undergoing transition. In the localised mode approximation, the in-phase motion of the nearest-neighbor alkali ions about their equilibrium position changes the total energy of the electron which is assumed to be localized in the anion vacancy. A parameter Q known as the configuration coordinate measures the displacement of the ions from equilibrium. The potential energy of the F-center electron is then plotted as a function of the configuration coordinate for both ground and excited states, after the manner for diatomic molecules. The Franck-Condon principle is then applied to the absorption and emission processes

of the electron, as shown in Fig. 1.

The F-center model has been used to treat the imperfection consisting of an impurity atom in a polycrystalline rare gas solid. Weyhmann and Pipkin* have studied the resonance absorption of matrix-isolated alkali atoms.

*Weyhmann, W. and Pipkin, F.M.: Phys. Rev. 137, A490 (1965).

The absorption spectrum consisted of one or two triplets, with the second triplet shifted considerably to the blue of the resonance lines of the free atom.

A configuration coordinate analysis was applied to the impurity atom interacting with its nearest-neighbor rare-gas atoms. The line width and the energy shift were written in terms of a Lennard-Jones (impurity-matrix) pair potential (V) and the configuration coordinate (Q). From the experimental value of the line width for sodium isolated in argon, the equilibrium coordinate Q_o was evaluated. The calculations indicated to the authors that the sodium atom may have been trapped not in a perfect substitutional site but in the vacancy created by two missing nearest-neighbors. This results in a site of only two-fold symmetry. The observed triplet splitting was then assumed to be due to the effect of the crystal field of the rare gas on the excited P state of the alkali atom.

Further work on this problem was done by Kupferman and Pipkin* who

*Kupferman, S.L., Pipkin, F.M.: Phys. Rev. 166, 207 (1968).

studied more closely the optical properties of rubidium atoms trapped in an argon matrix. They extended their studies to include measurements of

the ESR spectrum and the differential absorption of circularly polarized radiation by the samples. The ESR analysis led them to deduce that Rb atoms were trapped at three stable major sites. These sites were then assumed to be responsible for the different sets of triplets observed in the optical spectra. The separation between the two distinct sets of triplets was of the order of 1650 cm^{-1}. If Pipkin's explanation of multiple site effects is correct then the 3 major sites must be very different in their symmetry properties to produce such large shifts relative to one another.

The consistent occurrence of triplets in the spectra of trapped metal atoms having P ← S transitions in the gaseous state has been cited as evidence for the removal of the three-fold orbital degeneracy of the atomic P state by the asymmetric crystal field of the solvent. Britt and Schnepp*

---

*Schnepp, O., J. Phys. Chem. Solids, Pergamon (1961).

Brith, M. and Schwepp, O.: J. Chem. Phys. 39, 2714 (1963).

---

have studied both experimentally and theoretically the $^1P_1 \leftarrow {}^1S_0$ transition of magnesium trapped in argon, in an effort to throw some light on the possible mechanism of this removal of l-degeneracy. The contribution to the splitting was divided into two parts (a) the short-range covalent interactions between the valence electrons of the Mg atom in the excited (3s 3p) state and the outer-shell electrons of nearest-neighbor argon atoms in their ground states (b) the long-range dispersion interactions resulting from the polarization of the solute by the induced-dipole of the solvent. Although the crystal structure of argon is face-centered cubic (fcc) the calculations were done first for a distorted octahedral (Jahn-Teller)

environment and then for a vacancy in an otherwise regular octahedral site. The calculations predicted the splitting of the P state into two components instead of the observed three components. However, the splittings were of the right order of magnitude.

It is clear that the theoretical treatment of matrix effects is still in the embryonic stage.

C. Vapor Phase Spectra of the Noble Metals

The ground state electron configuration of the atoms of the noble metals can be written as $(n-1)\ d^{10}\ ns^1$ ($n = 4, 5, 6$) which gives rise to a $^2S_{1/2}$ ground state in LS notation. $^2P_{3/2,1/2}$ excited states arise from the $(n-1)\ d^{10}\ np^1$ configuration and their location about the ground state are shown in Table I, the values of which are taken from Moore.* Although the atomic states of gold have been designated in LS notation the AuI spectrum exhibits jj-coupling more closely.

*Moore, C. E.: Atomic Energy Levels NBS Circular 467 (1952).

Budick and Levin* have suggested that configuration interaction between the ^2P terms arising from the configurations $d^{10}p$ and d^9sp may be occurring. In copper and gold the perturbing ^2P states arising from the configuration $d^9\ sp$ are relatively close (Au $d^9sp\ ^2P_{3/2}$ 58,845 cm^{-1}) to the $d^{10}\ p\ ^2P$ states. Budick et al. therefore suggest that considerable mixing of the configurations may be expected to occur and that this mixing probably accounts for the enhanced intensity of the gold atomic line corresponding to the

*Budick, B., Levin, L.: Collog. Int. Centre Nat. Rech. Sci. 164, 195 (1966).

Table I.

A. Energy levels of atoms of the noble metals.

Configurations	States	Cu (n = 4) ν_0 (cm^{-1})	Ag (n = 5) ν_0 (cm^{-1})	Au (n = 6) ν_0 (cm^{-1})
$(n-1)\,d^{10}\,ns^1$	$^2S_{1/2}$	0	0	0
$(n-1)\,d^{10}\,np^1$	$^2P_{1/2}$	30,535	29,552	37,359
	$^2P_{3/2}$	30,783	30,473	41,174
$(n-1)\,d^{9}\,ns^2$	$^2D_{5/2}$	11,203	30,242	9,161
	$^2D_{3/2}$	13,245	34,714	21,435

B. Diatomic/atomic intensity ratios in the mass spectrometric studies of Cu, Ag, Au.

Element	Temperature range K	$(X2/X)\times 10^4$
Cu	1440 - 1560	4 - 10
Ag	1260 - 1360	5 - 8
Au	1500 - 1610	4 - 7

transition $d^{10}p\ ^2P \leftarrow d^9\ s^2\ ^2D$. In silver where the configurations are widely separated in energy (d^9 sp ^2P 65, 986 cm^{-1}) less mixing will undoubtedly occur. Budick still predicts an admixture of between 4 and 6 percent.

The close proximity in energy of the $d^{10}p\ ^2P$ and $d^9\ s^2\ ^2D$ states of Ag may result in admixture. Theory shows however that such perturbations can occur only between terms which have equal J and for LS coupling equal L and S. External pertubations like electric and magnetic fields may cause however a breakdown in these conditions and allow considerable admixing of the states.

The first doublet of the principal series of the silver atom ($5p\ ^2P_{3/2,1/2} \leftarrow 5s\ ^2S_{1/2}$) occurs at λλ 338.286 and 328.066 nm and both lines are quite strong. Cunningham and Link* have measured the lifetimes of the

*Cunningham, P., Link, J.: J. Opt. Soc. Am. 57, 1000 (1967).

$^2P_{3/2}$, $^2P_{1/2}$ states by the phase-shift method and arrived at values of 6.7 ns and 7.5 ns respectively. The calculated f-values are 0.481 and 0.287 for the transitions $5\ ^2P_{3/2,1/2} \leftarrow 5\ ^2S_{1/2}$. Bialas-Zabama et al* have made

*Bialas-Zabana et al: Acta Physica Polonica 19, 241 (1966).

some theoretical calculations of strength relations of doublet components of the principal, sharp and diffuse series of Cu I, Ag I and Au I. The values of S_2/S_1 (where S_2 is the line strength of $n\ ^2P_{3/2} \leftarrow n\ ^2S_{1/2}$ and S_1 the strength of line $n\ ^2P_{1/2} \leftarrow n\ ^2S_{1/2}$) are Cu I: 1 . 996: Ag I: 1.980; AuI: 1.948.

The absorption spectrum of silver vapor was photographed by Shin-Piaw*

*Shin-Piaw, C., Loong-Seng, W.: Nature 204, 276 (1964).

following vaporization of pure silver in a quartz tube containing argon or neon as a filling gas and heated by an electric furnace to temperatures below 1500 K. The doublet $\lambda\lambda$ 338.3 and 328.1 nm showed up very strongly at temperatures above 975 K. A weak doublet, assigned as the second doublet of the principal series ($6\,^2P_{3/2,1/2} \leftarrow 5\,^2S_{1/2}$) appeared above 1275 K. In addition a very faint band system was seen in the region 410.0 to 460.0 nm and was attributed to Ag_2. From these observations it was concluded that the equilibrium vapor of silver was made up almost entirely of monomer with very small amounts of dimer appearing above 1275 K.

The blue band system supposedly due to Ag_2 had been reported earlier by Kleman and Linkvist*. A King furnace was charged with silver metal

*Kleman B., Lindkvist, S.: Arkiv for Fysik 9, 385 (1955).

and heated to temperatures in the range 2000-2100 K. The band spectrum was studied in both emission and absorption and its assignment to Ag_2 was confirmed by isotopic substitution. Kleman and Lindkvist concluded from the vibrational analysis of the band system in emission that predissociation was probably occurring in the upper state (which they labelled A), whose vibrational frequency was estimated as 154.6 cm^{-1}. The lower state was presumed to be the ground state (X) with a vibrational frequency of 192.4 cm^{-1} and dissociation energy D_o of 14,520 cm^{-1}.

Kleman et al.* also studied the emission spectrum of copper and gold

*Kleman, B., Lindkvist, S.: Arkiv For Fysik 8, 505 (1954).

Kleman, B., Lindkvist, S.: ibid 8, 333 (1955).

in the King furnace. The copper emission consisted of an extended green system (designated A-X of Cu_2) from about 485.0 - 575.0 nm and a shorter blue system (B-X) from 450.0-470.0 nm. The dissociation energy of the ground state was estimated as 16,420 cm^{-1} and its vibrational frequency 266.1 cm^{-1}. With gold the emission spectrum extended from 4800-6400 A with ω_e'' = 190.5 cm^{-1} and D_o = 21,780 cm^{-1}.

Shin-Piaw* studied further the emission band systems of diatomic silver

*Shin-Piaw, C., Loong-Seng, W., Yoke-Seng: Nature 209, 1300 (1966).

in a discharge tube. Altogether six systems were observed, including the visible band system from 410.0-470.0 nm previously studied by Kleman et al. Shin-Piaw et al. obtained vibrational constants for the visible system which were in good agreement with Kleman et al. However they questioned Kleman's assignment of the lower state of this system as the ground state of Ag_2. Instead, their analysis of an ultraviolet system in the region 275.0-288.0 nm led them to believe that the lower state of this system was the ground state with a fundamental vibrational frequency of 207 cm^{-1} and not 192.4 cm^{-1}.

An interesting result of the discharge tube experiments was the detection of a new system in the ultra-violet from $\lambda\lambda$ 315.0-363.0 nm. This consisted of two strong winged bands centered about the atomic lines 328.07 nm and 338.29 nm and flanked by patches of weak continua. The bands were assumed to arise from an unstable upper state and an unstable lower state of Ag_2 resulting from Ag ($^2P_{1/2,3/2}$) + Ag $^2S_{1/2}$. The patches of continua probably originated from weakly bound Ag_2 or AgNe molecules.

D. Pressure Effects on the Resonance Lines of Silver

Clayton and Ch'en* studied the shift and broadening of the

*Clayton, E.D., Ch'en, S.Y.: Phys. Rev. 85 (1), 68 (1952).

$^2P_{3/2,1/2} \leftarrow {}^2S_{1/2}$ lines of silver due to the presence of argon and helium as a function of pressure.

They found that for argon both the λ 338.2 nm ($^2P_{1/2}$) and λ 328.0 nm ($^2P_{3/2}$) components were shifted to the red and broadened, with the $^2P_{1/2}$ experiencing a larger shift (about 5 cm^{-1} at 70 atm) and a larger broadening. On the contrary helium caused a shift to the blue in both components which were simultaneously broadened to about the same extent. Argon also produced a slight asymmetry towards the red while with helium a small asymmetry towards the blue was observed.

E. Mass Spectrometry of Noble Metals

The vapor over the condensed phase of copper, silver and gold at elevated temperatures is now known to consist predominantly of monatomic species. The composition shown in Table I were obtained in the mass spectrometric studies by Drowart and Honig*. Very small amounts of the trimer and

*Drowart, J., Honig, R.: J. Chem. Phys. 25, 581 (1956).

tetramer probably exist at these high temperatures and their upper limits have been estimated by Schissel*.

*Schissel, P.: J. Chem. Phys. 26, 5 (1957).

F. Low-Temperature Studies of Silver Atoms

Brown and Dainton* γ - irradiated Ag_2SO_4 - H_2SO_4 glasses at 77 K, and

*Brown, D.M., Dainton, F.S.: Trans. Fara. Soc. 62, 1139 (1966).

observed a strong absorption at λ 350 nm. Furthermore an absorption appearing as a shoulder at about λ 313 nm at 77 K increased in intensity on warming to 146 K as the main absorption decayed. They interpreted these results to mean that the 313 nm band probably originated from Ag atoms formed by reduction of Ag^+ ions by electrons generated by γ - irradiation of the matrix.

Zhitmikov* studied optically the products of the X - irradiation of

*Zhitmikov, R.A.: Opt. Spekt. 24 (1), 106 (1968).

aqueous and alcoholic solutions of some silver salts at 77 K. In treated AgF, $AgNO_3$ and $AgClO_4$ solutions, a broad band centered at about λ 395 nm appeared in each case and was assigned to $^2P \leftarrow {}^2S$ transitions of silver atoms. ESR spectroscopy also confirmed the presence of silver atoms in the X - irradiated samples.

Zhitnikov et al.* had studied earler the ESR spectrum of silver atoms

*Zhitnikov, R.A., Kolesnikov, N.Y., Kosyakov, V.I.: J. Exptl. Theoret. Phys. (U.S.S.R) 43, 1186 (1962).

trapped in non-polar hydrocarbons at 77 K. The silver atoms were produced by vaporization of the metal from an electrically heated molybdenum coil. The ESR absorptions of the trapped Ag^{107}, Ag^{109} atoms were seen to

be quite close to those of the free atoms. Each isotope further gave two ESR spectra with two different values of $\Delta\nu$ and g_J and this was cited as evidence for the existence of two types of trapping sites.

III. EXPERIMENTAL

A. Summary

Basically, an atomic beam of noble metal is generated in a Knudsen cell which is either resistance- or electron-bombardment heated. The inert matrix gas, introduced via a gas-handling system into the cryostat, is codeposited with the atomic beam on a sapphire target which has been cooled to 20 K by liquid hydrogen. The ultraviolet absorption spectrum of the solid solution is then photographed with a Jarrell-Ash spectrograph. An overall view of the equipment used is shown in Fig. 2.

B. Details

1. Cryostat

Experiments were conducted on the conventional metal cryostat shown in Fig. 3. The outer shell is made of brass and the inner dewar (A) of stainless steel. The pump-out port (V) for the cryostat is connected through a ball valve to a metal cold trap, then to a two-inch oil diffusion pump. The diffusion pump is backed by a three-phase motor rotary pump.

The stainless steel dewar is soldered at its base to a cylindrical copper block (E). A sapphire plate (40 mm × 20 mm × 3 mm) is clamped in a copper target holder (F) between indium gaskets to ensure proper thermal contact. The target temperature is measured by a germanium thermistor (G) (from Texas Instruments, Inc.) screwed directly onto the target. The thermistor was factory-calibrated in the temperature range 20 to 40 K. Its output is coupled to a chart recorder so that temperature changes can be monitored continuously. With liquid hydrogen in the dewar, the lowest target temperature recorded by the thermistor is 37 K.

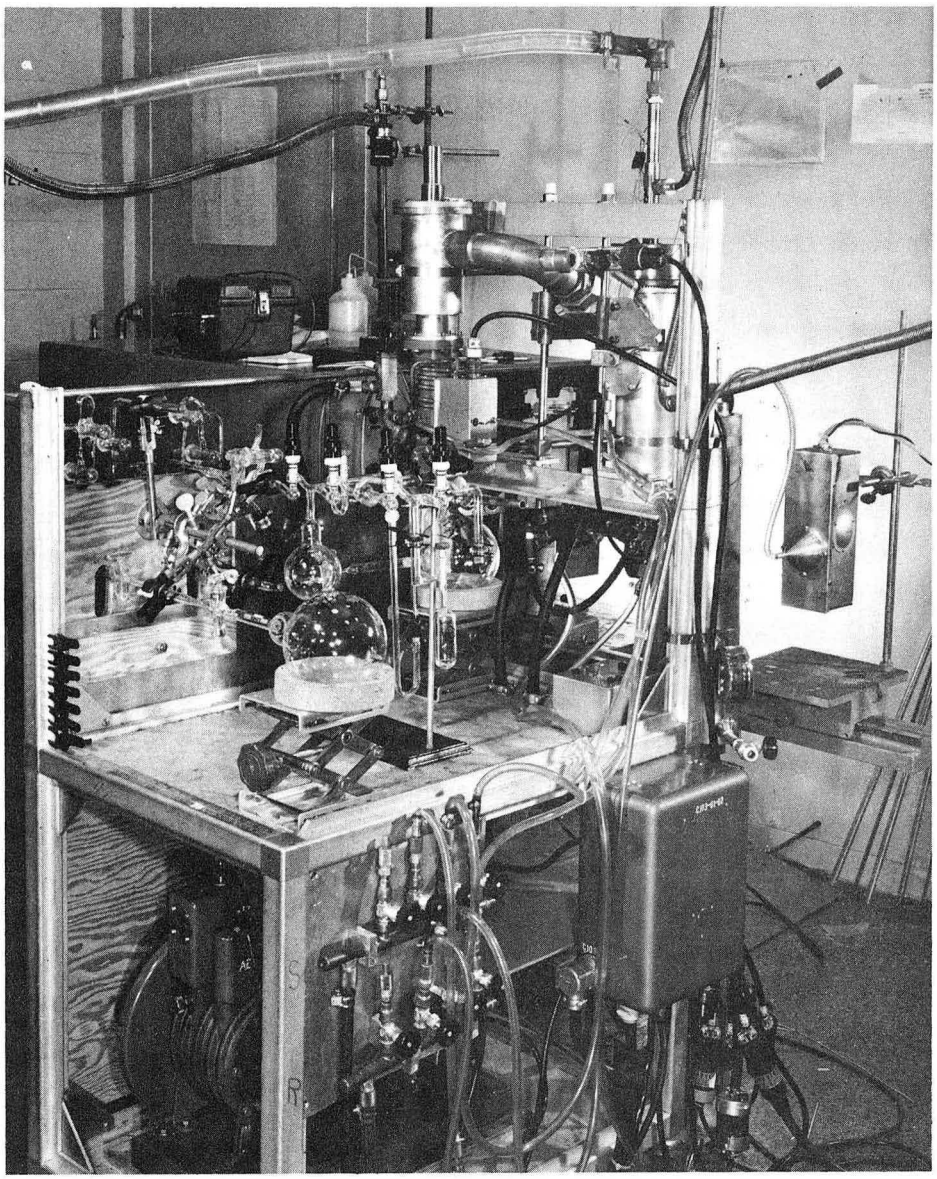

CBB 682-883

Fig. 2. Matrix isolation apparatus

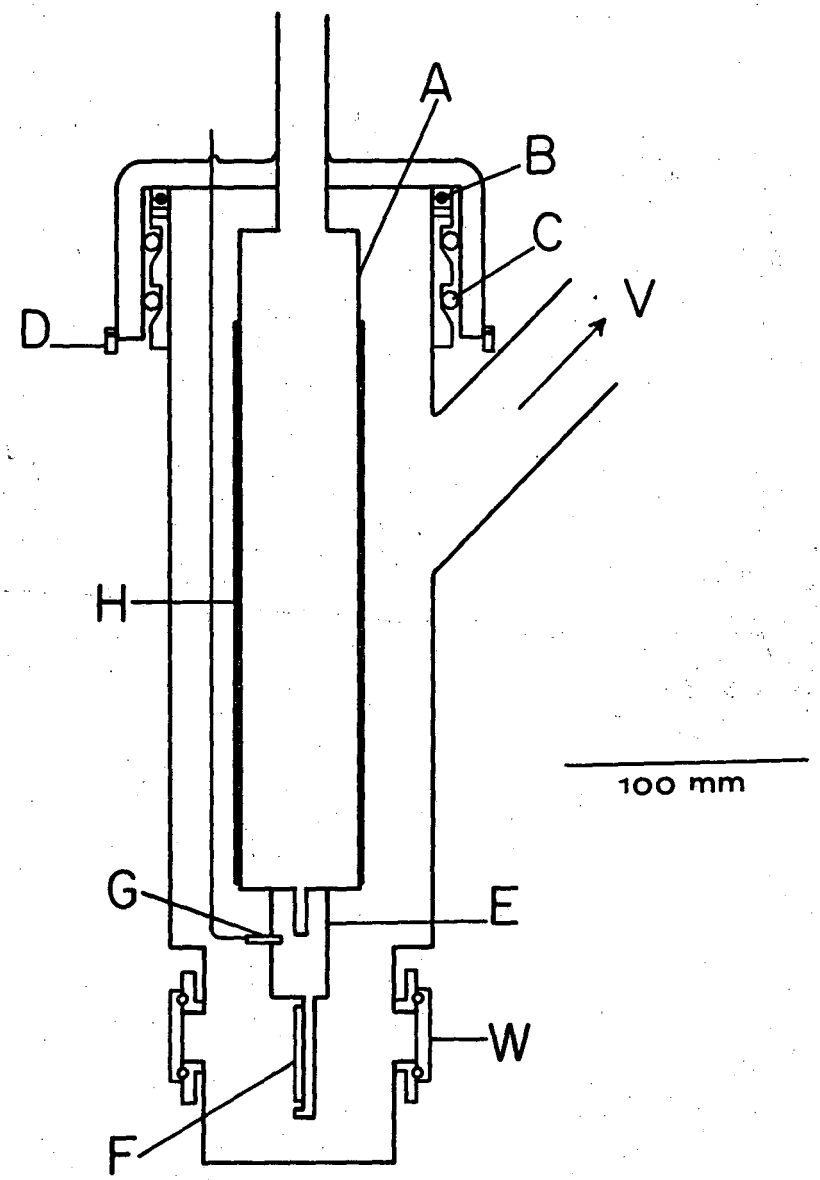

XBL 6810-6066

Fig. 3 Metal cryostat

It is possible the thermistor was not functioning properly or was lacking good thermal contact with the sapphire plate. If this were not the case, the large temperature gradient across the copper block could explain the difficulty experienced in isolating silver in argon (m pt. 84 K).

Because of the relatively large heat of vaporization of liquid hydrogen (106 cal g^{-1}) adequate insulation was provided by wrapping the dewar with three layers of aluminized mylar foil (H), 0.025 mm thick. Typically the dewar which had a capacity of approximately 1500 cc had to be refilled once every four hours during an experiment. Four ports were cut at right angles to each other in the outer shell of the cryostat. Two collinear ports carried sapphire windows (W) which served as the optical paths in the photographing of transmission spectra. A third port admitted the atomic beam from a furnace observable through the fourth port containing a quartz disc. The thin matrix film is laid down with the sapphire plate facing the beam squarely. After deposition the dewar is rotated through 90 degrees on ball bearings (B) by means of a gear arrangement (D) and the spectra photographed.

2. High Temperature Cells

a. Carbon resistor. The resistance-heated furnace used to generate a beam of noble metal in the single-metal experiments was of the same design as that used by Brabson* in his matrix studies on C_2 and is shown in Fig. 4.

Brabson, G. D.: Ph.D. Thesis (1965), University of California, Berkeley, UCRL-11976.

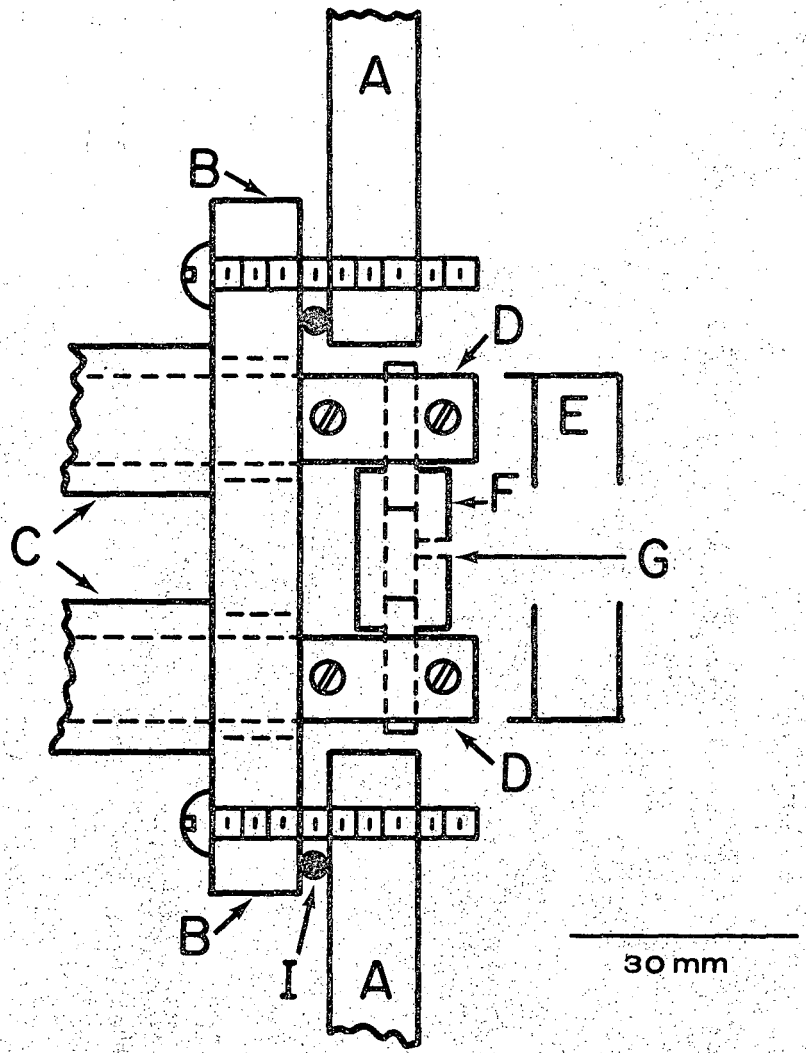

XBL 6810-6063

Fig. 4 Carbon resistance furnace

Here a Knudsen cell (F) replaced his Langmuir source. The cell was fabricated from spectroscopic purity graphite rod 6.5 mm in diameter. A 3 mm diameter hole was drilled lengthwise through the center of a 12 mm long segment of this rod and threaded internally at both ends. Two other pieces of graphite rod of diameter 3 mm were threaded externally and screwed into the ends of the hollow tube. These served as the contact points for the copper electrodes (D) passing through the brass flange (B) by means of the Kovar feedthroughs (C). In order to ensure good electrical contact with the jaws of the electrodes, the graphite end-rods were wrapped with deformable copper foil of 0.05 mm thickness. An effusion hole (G) 1 mm in diameter was drilled radially through the tube and midway along its length. The carbon resistor was partially enclosed by a set of 3 radiation shields (E) carrying a 5 mm × 3 mm aperture for collimation of the beam issuing from the Knudsen cell to the cold target situated 50 mm away.

The carbon resistor was heated by means of a transformer capable of delivering a maximum of 5 volts and 115 amperes. A temperature of 1150 K was attained with 3 volts and 60 amps flowing through the cell. A disappearing filament optical pyrometer was sighted through the opening in the radiation shield in measuring the cell temperature.

b. Electron bombardment heated cell. For the purpose of vaporizing two noble metals simultaneously and independently in order to study possible solute-solute interaction in the matrix, a simple, compact furnace assembly was needed. Electron bombardment heating of graphite Knudsen cells proved entirely adequate. The apparatus is shown in section

in Figs. 5 and 6. Two pure tungsten ribbon filaments (E) each of dimensions 30 mm × 0.75 mm × 0.025 mm were spot-welded to three tungsten support rods (B) 1 mm in diameter which were first capped with tantalum foil. Two of these support rods served as current leads through which typically 7 volts and 8 amps were passed while the third rod was grounded. All three rods exited through the brass flange by means of electrically-insulated Kovar-porcelain feedthroughs. The electrons generated by the heated filament were accelerated towards the graphite Knudsen cell by the application of a large positive voltage.

The graphite cell (F) was screwed onto the threaded end of 6 mm diameter tantalum rod. Because of the difficulty of hard-soldering the tantalum rod to the Kovar lead through, the tantalum rod was fused to a short piece of nickel tubing of the same diameter and this was in turn hard-soldered to the Kovar lead through. A positive potential was applied to this nickel-tantalum-graphite combination (A) from a regulated DC power supply capable of delivering 1000 volts and 500 milliamps. The Knudsen cell and tungsten filaments were enclosed by three concentric cylindrical tantalum radiation shields (D) with dimples to reduce conductive heat losses. The ends of this composite radiation shield were closed with 1.5 mm thick tantalum discs. Its base was pinned to three tantalum support rods (C) 1 mm in diameter which were screwed into the brass flange. A 6.4 mm diameter aperture in the radiation shield served to collimate the atomic beam from the Knudsen cell to the cold target.

Before operation the filaments and radiation shields were grounded. Then typically 7 volts and 8 amps were sent through the filaments. The maximum steady state temperature attained by radiation heating alone was

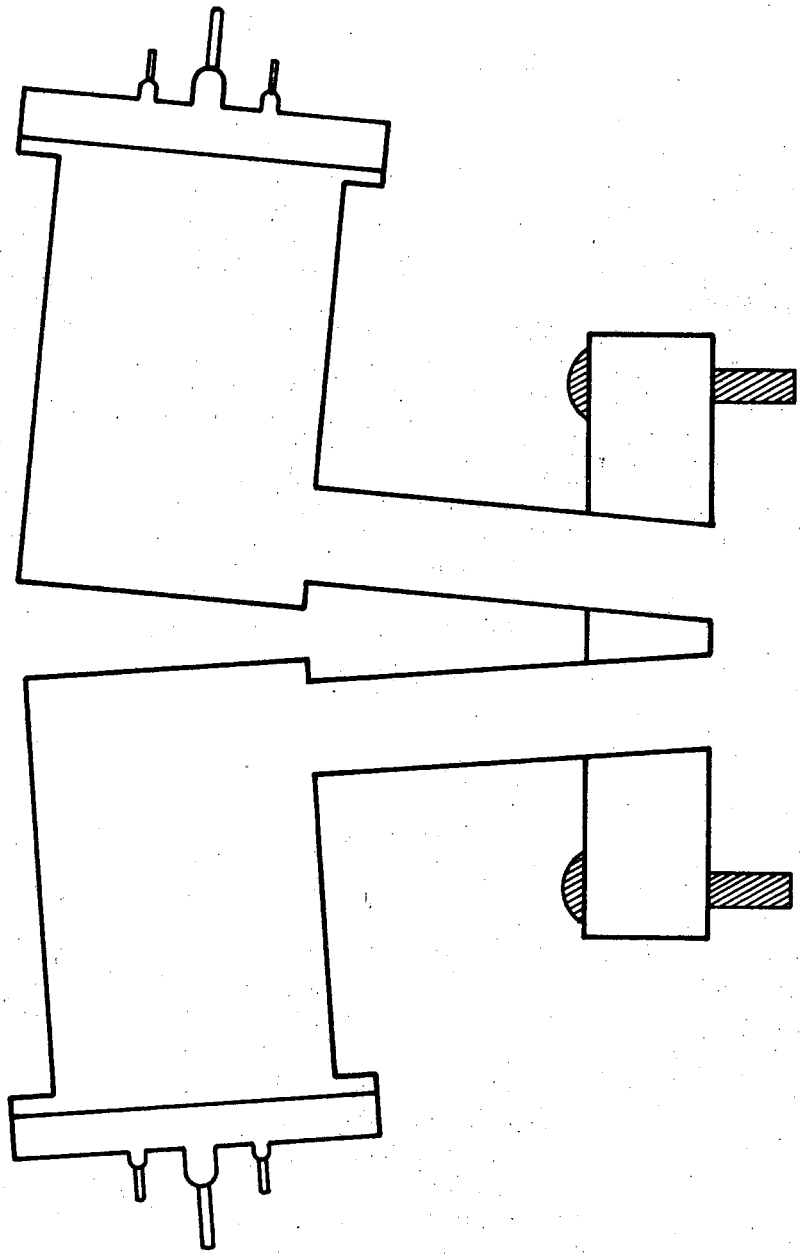

XBL 6810-6062

Fig. 5 Double beam arrangement of electron bombardment heated cells

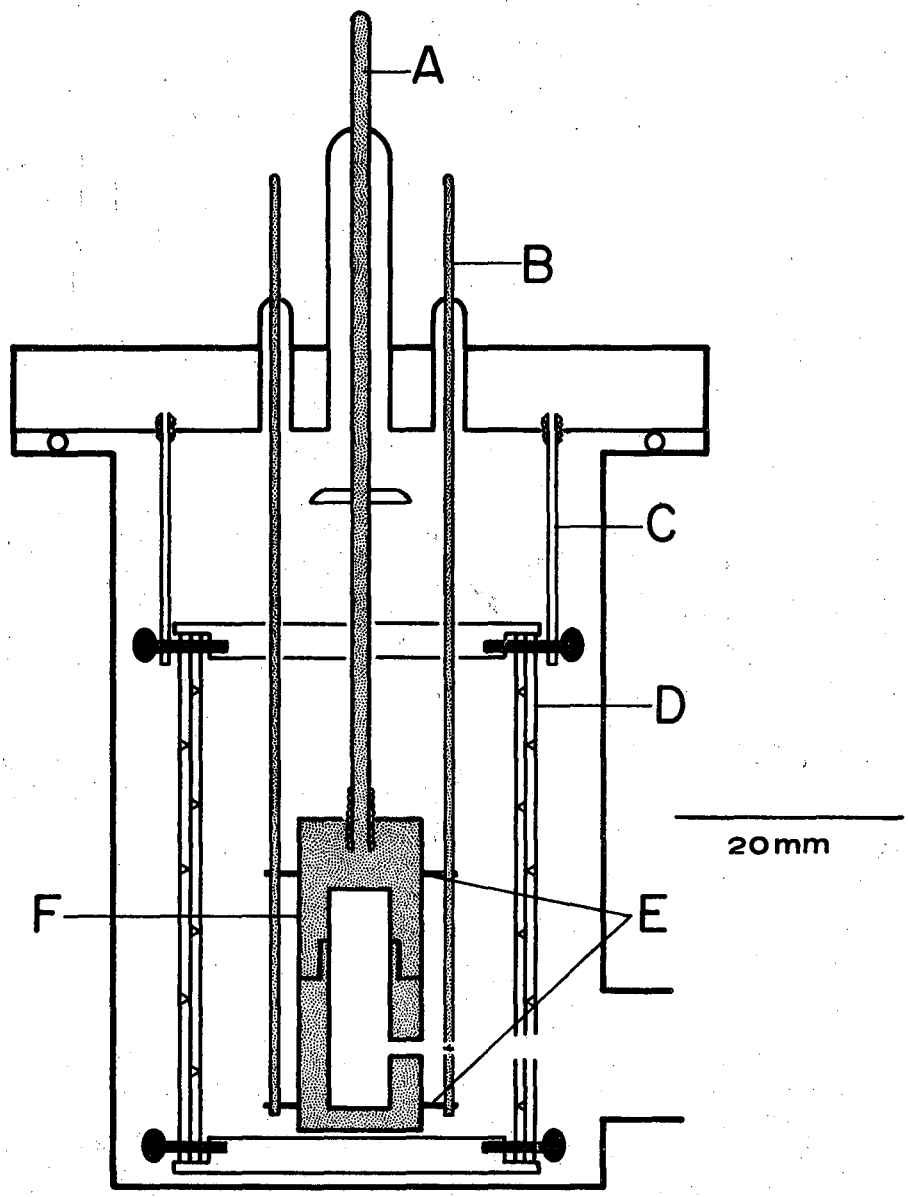

XBL 6810-6067

Fig. 6 Electron bombardment heated graphite cell

about 1100 K. For higher temperatures an accelerating voltage in the range 500 to 800 V was applied. The (bombardment) current flowing through the graphite cell was strongly controlled by the filament current and less so by the applied voltage. A steady-state temperature of about 1350 K was obtained with a positive potential of about 700 volts and a bombardment current of 150 mA. With care, temperatures could be maintained to within ±10 C, without any special controls on the filament current.

c. Estimation of metal concentration. The mass rate of efflux of the metal vapor through the orifice of the high temperature cell is estimated by applying the ideal Knudsen equation:

$$\frac{dm}{dt} = P \sqrt{\frac{M}{2\pi RT}}$$

where m is the mass in grams of vapor issuing from the orifice in time t seconds, P is the equilibrium vapor pressure in atmospheres inside the cell, M is the gram-molecular weight of the species, and T the absolute temperature in degrees Kelvin.

By integrating over a time t, the number of g-moles R issuing from an orifice of area a mm^2 is given by

$$R = (4.43 \times 10^3) \frac{P \cdot a \cdot t}{\sqrt{MT}}$$

The usual simplifying assumptions implicit in the use of Knudsen's equation, for example the existence of thermodynamic equilibrium and the absence of hydrodynamic streaming through the orifice, are adopted here. No attempt has been made to assess the degree to which our experimental

conditions deviate from ideality. Furthermore these values of R obtained by the Knudsen equation are not corrected for the fraction f of the atomic beam intercepted by the cold target and the condensation coefficient α. α is probably close to unity. With the dimensions existing in our system a rough calculation using the cosine law of evaporation shows that probably less than 10 percent of the effusate is collected by the target.

Metal vapor pressures varied usually between 5×10^{-4} and 1×10^{-3} torr.

3. Gas Handling System

A dual channel system similar to the one used by Brabson* handled

---

* Brabson, G. D.: Ph.D. Thesis (1965) University of California, Berkeley, UCRL-11976.

---

the matrix gases entering the cryostat. Leak rates were regulated by precision Nupro needle valves and monitored by calibrated Fischer-Porter flow meters equipped with sapphire floats. Tube sizes were either 3.2 mm or 1.6 mm depending on the quantity of gas to be delivered. Typical leak rates were of the order of 0.5 millimoles per hour.

Gas mixtures were prepared by successive condensation of the components into a 200 ml bulb immersed in liquid nitrogen. The mixture was warmed slowly to room temperature and allowed to equilibrate for at least 18 hours before use.

The number of moles (M) of gas used in a particular experiment was estimated by means of the ideal gas equation

$$M \equiv n = RT/p'v$$

The pressure in the bulb of known volume V (usually 1 liter) was measured by a mercury manometer at the beginning and end of deposition. The difference p' was inserted in the ideal equation. In the case of matrix materials which were liquid at room temperature the vapor pressure was used in the equation.

4. Heat Transfer Analysis

The rate of heat removal from the target is an important factor controlling the efficiency with which the atoms are trapped. The relatively high thermal conductivity of the sapphire plate (0.85 cal $mm^{-1}sec^{-1}K^{-1}$) is an asset in this respect and so is the large refrigeration capacity of the liquid hydrogen dewar. A few simple calculations have been made to determine the heat input to the target that must be accommodated. Let us consider for example an actual experiment in which 1.4×10^{-7} moles of gold vapor at 1336 K and 7×10^{-4} moles of krypton at 293 K were codeposited on a sapphire plate at 20 K during 115 minutes.

The heat input to the target is assumed to come from two important sources. First there is heat (q_c) released by a change in the enthalpy of both the matrix gas (ΔH_M) and the impurity atom (ΔH_R) in being cooled from their initial to their final temperatures. Secondly there is the contribution q_r due to radiative transfer from the hot Knudsen cell.

For krypton if we approximate the heat of sublimation at 20 K to that at its melting point* then

$$\Delta H_M = \int_{293}^{20} C_p\,(g)\,dT + (\Delta H_S^o)_{20}$$

$$\approx (4.97)(273) + 2{,}570 = 3{,}926 \text{ cal mole}^{-1}$$

*Brewer, L: High Strength Materials, V. F. Zackay, ed. (John Wiley and Sons, Inc, New York, 1965) . .

or the heat q_c released by the krypton = $(3{,}926)(7 \times 10^{-4}) = 2.75$ cal. In estimating ΔH_R, we will assume that the heat of condensation of gold in krypton has as its upper limit the heat of sublimation of pure gold at the same temperature. The degree to which this is a valid approximation will depend on the tightness of the binding between gold and krypton molecules in the solid. Assuming also that the vapor over liquid gold is all atoms we have

$$\Delta H_R = \int_{1336}^{20} C_p(g)\, dT + (\Delta H_S^o)_{20}$$

$$\approx (4.97)(1316) + (87{,}300) = 93{,}840 \text{ cal mole}^{-1}$$

and the heat released by the gold vapor on condensation = $(93{,}840)(1.4 \times 10^{-7}) = 1.31 \times 10^{-2}$ cal. so that $(q_c)_{Kr} \gg (q_c)_{Au}$. It is seen then that, because the amount of matrix gas is large compared to gold ($M/R \approx 5 \times 10^3$) the solvent dominates the heat input due to condensation. Even at $M/R = 50$, it is more than twice as large. Krypton has been cited in this example. However, when polyatomics like SF_6 and fluorocarbons are employed as matrices the heat released is even greater due to rotational and vibrational contributions to the heat capacity. In such cases it is probably expedient to precool the gas.

The total radiant energy q_r emitted by a non-black body is given by the equation*

$$q_r = \sigma\, e\, A\, T^4$$

---

* Bird, R. B., Stewart, W. E. and Lightfoot, E. N.: Transport Phenomena, (John Wiley and Sons, Inc., New York, 1960).

where e is the emissivity of the surface, A is the area in mm^2, and T is the absolute temperature in degrees Kelvin. σ is the Stefan-Boltzmann constant = 1.355×10^{-14} cal sec^{-1} mm^{-2} K^{-4}. If we put e = 1 for the graphite and sapphire surfaces, then the radiant energy impinging on unit area of the sapphire plate in unit time is calculated to be of the order of 4×10^{-4} cal sec^{-1} mm^{-2} at the center of the plate.* This can be compared with the rate of heat input due to condensation which is about 5×10^{-8} cal sec^{-1} mm^{-2} if we assume that about 10% of the matrix gas entering the cryostat is collected by the cold target.

* See Appendix, this thesis

Because the thermal conductivity of the sapphire at 20 K (0.85 cal mm^{-1} sec^{-1} K^{-1}) is so much larger than that of copper at 20 K (0.31 cal mm^{-1} sec^{-1} K^{-1}) the heat admitted to the target is probably conducted away lengthwise from bottom to top. The temperature gradient across this length is calculated to be of the order of 0.13 K which is quite small. Other gradients probably involve the thermal resistances due to the copper holder, the indium gaskets, the solder connection between the copper block and the steel dewar, the dewar wall, the heat transfer coefficient inside the dewar. The last mentioned contribution has been roughly estimated to be about 3K for the heat flux calculated above. It is interesting to note that the germanium thermistor located near the center of the plate registered a temperature rise of 3.2 K on raising the furnace temperature from room to 1336 K.

5.. Optical Systems

Spectra were photographed with a Jarrell-Ash spectrograph having an effective focal length of 750 mm and an exit aperture ratio f/6.3. The plane grating (G) in the Czerny-Turner mounting scheme was blazed for

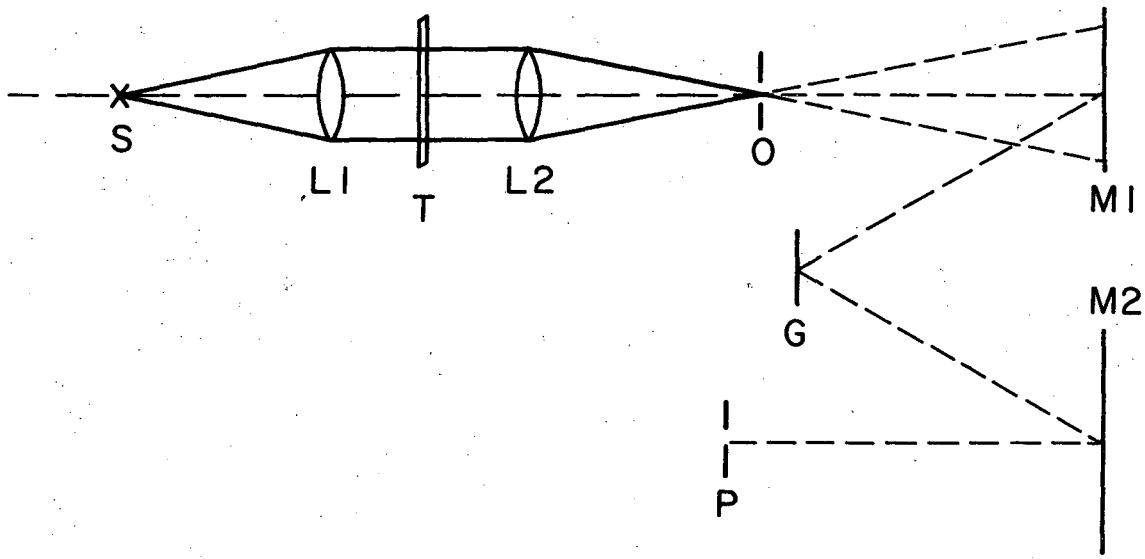

XBL 6810-6064

Fig. 7 Optical arrangement for absorption spectra in transmission

300 nm and had 2160 lines per mm. This gives a dispersion in the first order of 0.5 nm per mm.

Background continua for the ultraviolet were provided by a 150 watt xenon-mercury arc lamp operating at 8 amp. A 1-kilowatt hydrogen discharge lamp was also used, mainly in the study of gold below 250 nm. A medium pressure mercury discharge lamp served as the reference source. The optical arrangement for photographing absorption spectra is shown in Fig. 7. Radiation from the continuum source (S) reached the target (T) as parallel rays after passing through the positive quartz lens (L_1). The radiation leaving the target was collected by a second quartz lens (L_2) and focused onto the spectrograph slit (O). Spectral images were recorded on Kodak 103aO or SWR plates (P) following reflections by the concave mirrors (M_1) and (M_2) of the spectrograph. Slit widths normally employed were about 60μ, with exposure times ranging from 1/10 second to 5 minutes depending on such factors as the transmission characteristics of the matrix and the concentration of absorbing species.

Kodak 103aO plates were useful down to about 245.0 nm after which their sensitivity fell off rapidly. This accounts for the steepness of the background in many of the densitometer traces shown. Below 245.0 nm Kodak Shortwave Radiation (SWR) plates were superior in sensitivity. However extreme care had to be exercised in handling these plates because the emulsion would not withstand even mild fingerprinting or pressure.

Specular Reflectance Spectra were recorded in a few experiments on silver atoms. In this case the light source was focused through the window opposite the beam generator onto a highly polished aluminum target whose plane surface made an angle of 45° with the incident beam. The specularly reflected beam was collected by lens L_2 and focused onto the slit of the spectrograph.

Unsuccessful attempts were made to measure the resonance fluorescence spectrum of silver atoms trapped in krypton. The configuration adopted was close to that used in the specular reflectance experiments except that a transparent sapphire target replaced the aluminum target and was rotated 90°. In this way the reflected exciting light passed out of the system through one window while the 'fluoresced' light was collected from the opposite window and focused onto the spectrograph slit. The exciting radiation was selected from the output of an AH 6 high pressure mercury lamp by either a Bausch and Lomb monochromator or Jena μG 11 filter. Both photographic plate and photomultiplier (using RCA 1P28 Tube) detections were tried. In either case the scattered light problem made meaningful measurements impossible.

IV. RESULTS AND DISCUSSION

A. Silver

1. Argon

The trapping of silver species by argon was rather inefficient at 20 K, possibly because of the relatively low melting point (84 K) of argon. As a result, thick concentrated deposits were necessary in order to observe moderately strong absorptions. Three maxima are clearly discernible, however. The long wavelength component (ν_1) at 315.0 nm has a half-width at 20 K of the order of 350 cm^{-1} which becomes still greater as the temperature of the matrix is increased. One is tempted to correlate this transition to the $^2P_{1/2} \leftarrow {}^2S_{1/2}$ transition in the gas phase and this represents a considerable blue shift of 2195 cm^{-1}. This behavior is not unusual for argon which among the rare gases always seems to produce the largest blue shifts. The other two absorption maxima (ν_2) and (ν_3) located at 304.1 and 298.6 nm, respectively, give the appearance of a doublet structure. The upper states of these two transitions could well have originated from the $^2P_{3/2}$ state of the free atom. Again the blue shifts are seen to be considerable (2140 and 3015 cm^{-1} respectively). The half-widths of ν_2 and ν_3 are difficult to assess since they are not completely resolved but they are probably of the order of 400-500 cm^{-1}. These features also broaden and shift as the target temperature is raised. A fourth extremely weak absorption ν_4 occurs at about 331 nm and can only be observed after long deposition times. This feature remains essentially unidentified although one may speculate that it is probably due to silver dimer or to an impurity. We may note however that this band has no counterpart in the gaseous Ag_2 spectrum. Conversely

Table II. Absorption spectra of matrix-isolated silver at 20 K

Matrix	λ(nm)	$\nu(cm^{-1})$	Assignment	$\nu-\nu_0(cm^{-1})$
Argon (M/R = 400)	330.9 ± 1.0	30,221 (w)	?	
	315.0 ± 0.5	31,746 (s)	$^2P_{1/2} \leftarrow {}^2S$	+ 2,194
	304.1 ± 0.5	32,884 (m)	$^2P_{3/2} \leftarrow {}^2S$	+ 2,411
	298.6 ± 0.5	33,490 (m)		+ 3,017
Krypton (M/R = 150)	322.7 ± 0.5	30,989 (s)	$^2P_{1/2} \leftarrow {}^2S$	+ 1,437
	313.6 ± 0.5	31,888 (s)	$^2P_{3/2} \leftarrow {}^2S$	+ 1,415
	309.4 ± 0.5	32,321 (s)		+ 1,848
Xenon (M/R = 200)	334.6 ± 0.3	29,886 (s)	$^2P_{1/2} \leftarrow {}^2S$	+ 334
	327.3 ± 0.3	30,553 (s)	$^2P_{3/2} \leftarrow {}^2S$	+ 80
	325.7 ± 0.3	30,703 (m)	$^2D_{3/2} \leftarrow {}^2S$	- 4,011
	322.6 ± 0.3	30,998 (s)	$^2P_{3/2} \leftarrow {}^2S$	+ 525

the systems in the gas around λλ 440 and 280 nm which were assumed to involve the ground state were not observed in the matrix spectrum.

2. Krypton

The spectrum of silver trapped in krypton showed three very strong absorptions with comparable half-widths of the order of 250 cm^{-1} at 20 K. The structural pattern bears a close resemblance to that of argon except that in this case the doublet ν_2 and ν_3 is better resolved and not as blue-shifted, relative to the gas phase $^2P_{3/2} \leftarrow {}^2S_{1/2}$ transition (1415, 1848 cm^{-1}, respectively). The singlet ν_1 also experiences a smaller shift of +1437 cm^{-1} from the $^2P_{1/2} \leftarrow {}^2S_{1/2}$ transition of the free atom. All three bands show temperature effects of broadening and shifting. A fourth band, reported in an earlier paper (to be published) was absent in subsequent experiments and could have been due to impurity. It will not be reported here as part of the krypton matrix spectrum.

The above mentioned frequencies pertain to the absorption spectrum taken in transmission through a sapphire target. However, identical results are obtained from the specular reflectance spectrum of a thin film deposited on a highly polished aluminum target. The reflection technique would be particularly useful for matrix films like Xe, SF_6 which have poor transmission characteristics beyond a certain thickness.

A detailed study was made of the effect of the M/R ratio on the spectral pattern of silver isolated in krypton. Ratios were varied from about 100 to 4,000 by keeping the temperature of the silver in the Knudsen cell constant and changing the flow rate of the matrix gas. Also, a number of experiments of the same M/R were run by varying the deposition times and proportionately changing both the silver temperature and the

krypton flow rate. In all cases the three bands had roughly the same shape and same half-width. The occasional slight variation in the half width depended more on the optical thickness of the samples than on the M/R ratio. Because of the absence of any effect of M/R, in subsequent experiments a certain temperature (and hence vapor pressure) of the solute was selected and then the near-minimum amount of rare gas used. In this way the heat input to the target by condensation was minimized and so was the opacity of thin films like Xe and SF_6.

Detailed studies of the effect of annealing the matrix to different temperatures about 20 K were also done on the Ag-Kr system. The procedure involved the removal of the liquid hydrogen from the dewar and allowing the target to warm up spontaneously to a certain temperature (as monitored by the germanium thermistor) then quickly recooling to 20 K by reintroduction of liquid hydrogen. The spectrum was then photographed and the annealing process repeated but to a higher temperature. This was continued until a temperature was found where the absorption spectrum was no longer present. The purpose of this sort of experiment was two-fold, first to see whether polymers of silver could be formed by diffusion in the solid and secondly to examine the possible contribution of multiple sites in the original spectrum at 20 K. On warming to higher temperatures the peak absorptions shifted positions, mainly to the red and the half-widths increased markedly. However no new features appeared as the original spectrum decayed and this suggests that dimer formation and stabilization was not occurring. This is in contrast to the behavior of Li atoms in a rare gas matrix as reported by Andrews and Pimentel.* In their studies of

---

* Andrews, L. and Pimentel, G. C.: J. Chem. Phys. 47, 2905 (1967).

lithium isolated in krypton at 4 K, warming produced a new band which was assigned to an Li_2 transition. We can reconcile the two sets of observations if we postulate that the silver atom-rare gas interaction is quite strong compared to the Li-rare gas and rare gas-rare gas interactions. The fact that the Ag atom spectrum was still reasonably strong even when a fair portion of the matrix gas had been lost by evaporation at temperatures above 20 K, probably lends some validity to this interpretation. Eventually a temperature is reached where even these Ag-rare gas bonds are broken and rapid nucleation follows (in which case the dimer or trimer spectrum would not be observed). The strong interaction of the noble metal atoms with the rare gas is probably also reflected in the very large blue shifts observed for the system.

On warming to a temperature just below the point of disappearance of the original spectrum, the spectra taken on recooling showed no detectable change in the half widths of the three bands. One might argue that if atoms are deposited originally in two or more sites which have different thermodynamic stabilities, the annealing process should favor conversion to the most stable configuration. This apparently was observed to have been the case in the trapping of sodium by Meyer.* There, two sets of

---

Meyer, C. B.: J. Chem. Phys. 43, 2986 (1965).

---

triplets occurred and one disappeared on annealing. However, if annealing has no visible effect, as in our case, it does not necessarily follow that we are not dealing with a case of multiple sites. It could be that the two sites occur at thermodynamic equilibrium and even if $\Delta F < 0$ for the process the kinetics may be such that it does not take place in the relatively short duration of annealing. In view of these possibilities

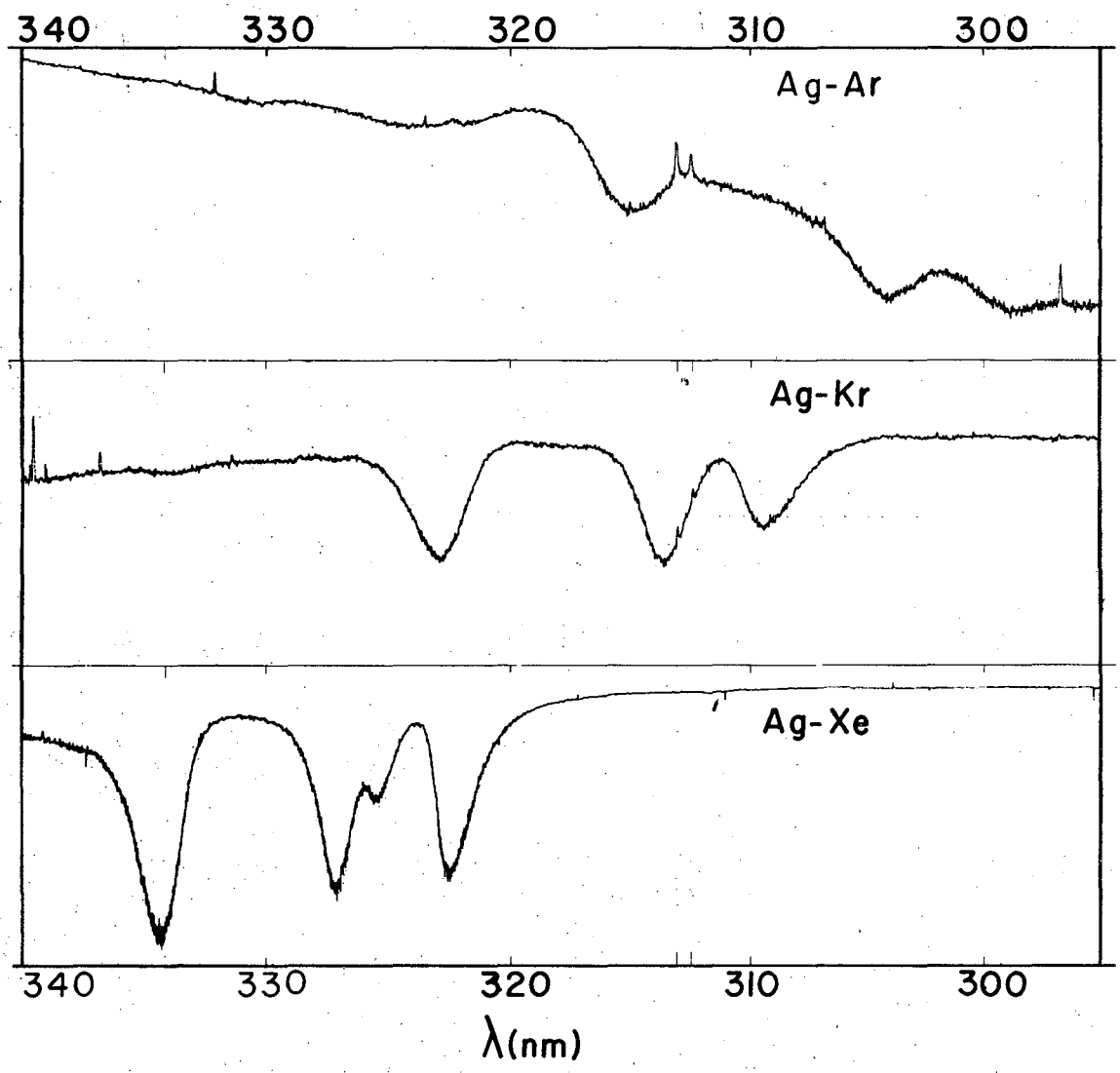

XBL 6810-6046

Fig. 8 Absorption spectra of matrix-isolated silver atoms

no definitive statements can be made on the contribution of multiple sites in the spectrum of silver in krypton.

3. Xenon

The isolation of silver atoms in xenon is extremely efficient; a Knudsen cell temperature of about 1140 K and a deposition time of 30 minutes being sufficient to give an intense absorption spectrum. Three strong transitions occur; the long λ component (ν_1) is blue-shifted with respect to the free atom $^2P_{1/2}$ state by 334 cm^{-1} while the 327.3 (ν_2) and 322.6 nm (ν_3) components are blue-shifted 80 and 525 cm^{-1} from the gaseous atom $^2P_{3/2}$ term. The separation between ν_2 and ν_3 (445 cm^{-1}) is comparable to that for krypton (433 cm^{-1}) but considerably less than that for argon (606 cm^{-1}). All three components in xenon have half-widths of about 200 cm^{-1} which are strongly temperature dependent. A fourth component (ν_4), though weaker than the other three, is present at all concentrations of silver studied (which is in contrast to the argon and krypton cases). This is clearly not due to impurity. Its correlation to a free atom term is not readily apparent unless one assumes the $^2D_{3/2}$ state situated at 34,714 cm^{-1} in the gaseous atom is mixed in with ^2P terms due to the presence of the polarized xenon molecules. The transition probability of this forbidden ($^2D_{3/2} \leftarrow {}^2S_{1/2}$) transition has not been measured in the gas phase but is expected to be very small. This fact, together with the large energy discrepancy (4,000 cm^{-1}) between the gas and matrix values makes such an assignment rather tenuous. It may be noted however that the copper atom in which the ^2D state is low-lying and not likely to mix with the ^2P state to any extent, shows only three absorptions in xenon in this spectral region.

4. Sulfur Hexafluoride

The absorption spectrum of silver cocondensed with SF_6 at 20 K has a diffuse, almost nondescript appearance. At low concentrations of silver two broad, weak contiguous bands with maxima at 333.0 and 329.0 nm are the only discernible features. As the concentration of silver builds up, these two bands become still broader while a patch of weak continuum joins onto the short wavelength end. (Prolonged deposition does not affect greatly the individual intensities although the integrated intensity is clearly increasing.) When the temperature of the matrix is raised, the short wavelength continuum region reduces in intensity but so does the long wavelength region. Recooling does not produce any noticeable enhancement of the intensities. In addition to the above mentioned features a broad but strong absorption band centered at about 214.5 nm occurs in the absorption spectrum of the film originally present at 20 K. It must also be remarked that no spectra are obtained when large amounts of SF_6 ($M/R > 200$) are used in the cocondensation process.

The interpretation of the absorption spectrum is not simple in the absence of more definitive studies like fluorescence. It seems however that the transition at 214.5 nm correlates fairly well with the free atom $6p\ ^2P_{3/2,\ 1/2} \leftarrow\ ^2S_{1/2}$ transitions at $\lambda\lambda$ 207.0 and 206.2 nm. (It may be remarked at this point that a search was made for these transitions in Ag atoms isolated in krypton and xenon. No bands were seen in the region bordering on the vacuum ultra-violet. Because these transitions seem to have fairly large f-values in the gaseous atom, the situation in the matrix is probably such that these are shifted into vacuum UV where they are not detectable with our spectrograph.) This suggests that at least some portion of the continuum absorption around 330.0 nm may be due to atoms. Alternatively, all or part of this continuum may be due to some molecular species

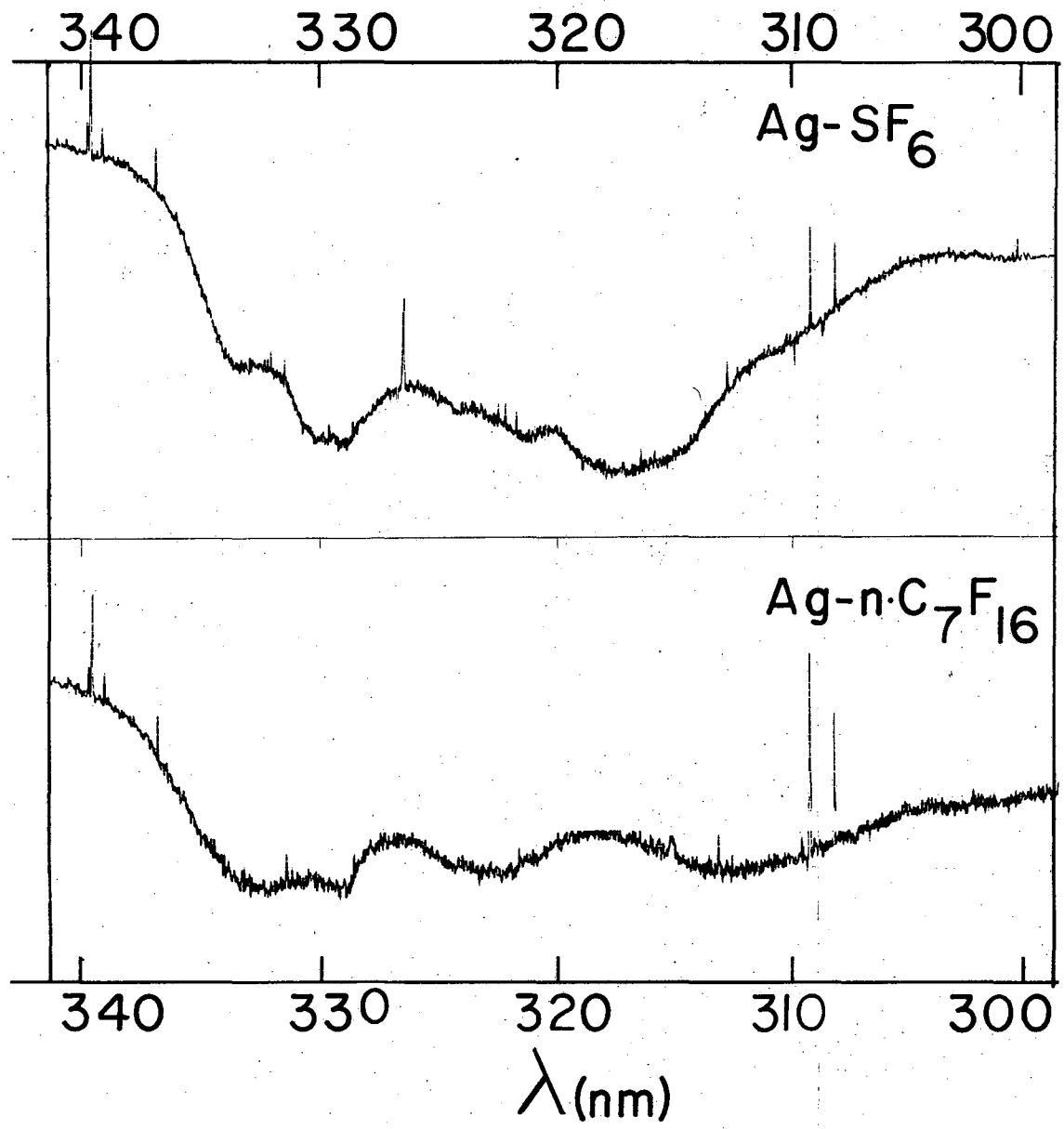

XBL 6810-6044

Fig. 9 Absorption spectra of silver cocondensed with fluoro compounds at 20 K.

like AgF formed by reaction either in the gas phase or on cocondensation.

$$Ag(g) + SF_6(g) \rightarrow AgF(g) + 1/2\ S_2F_{10}(g)\ \Delta H \approx -24 \text{ kcal}$$

The absorption spectrum of AgF vapor has been measured recently by Clements and Barrow.* They report that the strongest feature is a continuum

* Clements, C. and Barrow, R. : Chem. Commun. 1, 27 (1968).

centered at about λ 303.0 nm with the $B \leftarrow X$ and $A \leftarrow X$ systems occurring at longer wavelengths. At $\lambda < 260.0$ nm a third system $C \leftarrow X$ occurs. It is tempting to correlate the Ag-SF_6 matrix absorptions to the AgF(g) systems but $Ag_2(g)$ also has absorptions in this region as do Ag atoms. However, it should be possible to trap AgF vapor (in equilibrium with AgF solid) in a matrix of krypton or xenon, then compare its spectrum with that obtained by cocondensing silver and SF_6.

5. n-C_7F_{16}

The spectrum of silver cocondensed with n-C_7F_{16} vapor shows a weak continuum centered at about λ 310.0 nm. Five weak but discrete bands also occur at $\lambda\lambda$ 268.7, 258.8, 252.7, 246.9, and 236.8 nm. This spectrum remains unidentified. Comparison with Ag-SF_6 suggests the possibility of a common absorbing species such as AgF.

B. Copper

1. Krypton

The absorption spectrum of copper in a krypton matrix shows three main bands of comparable peak intensities. At 20 K the bands are quite broad with half-widths of the order of 450 cm^{-1}. This broadness probably accounts for the weak overall appearance of the spectrum even after prolonged deposition at temperatures as high as 1350 K. The half-widths do not change when the matrix is warmed and recooled to 20 K. The

separations between successive maxima are equal (375 cm^{-1}) within experimental error. A correlation with the free atom spectrum on the same basis as that for silver shows that the $^2P_{1/2} \leftarrow {}^2S_{1/2}$ transition is blue-shifted by 1230 cm^{-1} while the $^2P_{3/2}$ components are shifted 1360 cm^{-1} and 1736 cm^{-1} to the blue. These shifts are of the same order of magnitude as those occurring in silver. At higher concentrations of copper, an additional weak band occurs at about 325.5 nm and is probably due to Cu_2, although no such band has been reported for gaseous Cu_2. Furthermore the Cu_2 (g) visible systems were not observed in the matrix spectrum of copper.

2. Xenon

Three very intense absorptions are the main features of the spectrum of copper isolated in a xenon matrix. The wavelengths listed in the table were obtained in an experiment in which the M/R ratio was about 50. Mercury atoms were also accidentally present as a contaminant. The general appearance of the triplet is similar to that for krypton, but all the components suffer smaller blue shifts with respect to the gas values. Half-widths are of the order of 300 cm^{-1}. The higher energy transitions listed may be due to Cu polymers in view of the low M/R used. They may also be correlated to 'forbidden' transitions involving ^4P and ^4D terms of the atom.

3. SF_6

At fairly high concentrations of copper in sulfur hexafluoride, the absorption spectrum consists of a strong continuum centered at approximately 315.0 nm and extending over a 17 nm-wide region. When the matrix

Table III. Absorption spectra of matrix-isolated copper at 20 K

Matrix	λ(nm)	$\nu(cm^{-1})$	Assignment	$\nu-\nu_0(cm^{-1})$
Krypton (M/R = 250)	325.5 ± 0.5	30,722 (w)	?	
	314.8 ± 0.5	31,766 (m)	$^2P_{1/2} \leftarrow {}^2S$	+ 1231
	311.1 ± 0.5	32,144 (m)	$^2P_{3/2} \leftarrow {}^2S$	+ 1360
	307.5 ± 0.5	32,520 (m)	$^2P_{3/2} \leftarrow {}^2S$	+ 1736
Xenon (M/R = 50)	326.3 ± 0.5	30,647 (s)	$^2P_{1/2} \leftarrow {}^2S$	+ 112
	323.7 ± 0.5	30,893 (s)	$^2P_{3/2} \leftarrow {}^2S$	+ 109
	320.1 ± 0.5	31,240 (s)	$^2P_{3/2} \leftarrow {}^2S$	+ 456
	283.1 ± 1.5	35,323 (w)	?	
	273.5 ± 1.5	36,563 (w)	?	
	266.4 ± 0.5	37,538 (w)	?	
	248.5 ± 0.5	40,241 (w)	?	
	247.0 ± 0.5	40,486 (w)	?	
SF_6 (M/R = 100)	319.0 ± 1.0	31,348 (s)	?	
	312.5 ± 1.0	32,000 (s)	?	
	242.5 ± 0.5	41,237 (m)	?	
	237.4 ± 0.5	42,123 (m)	?	

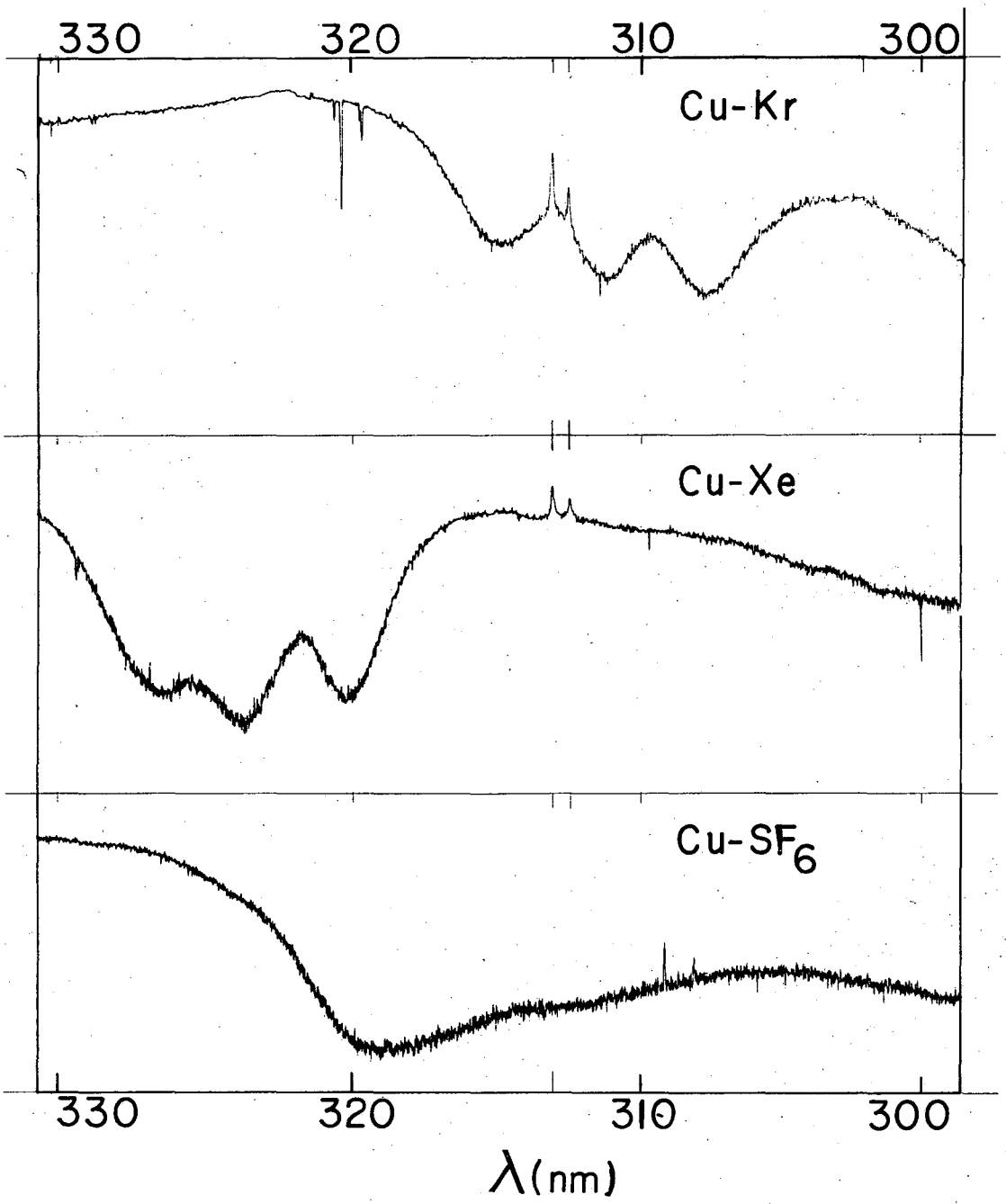

XBL 6810-6042

Fig. 10 Absorption spectra of matrix-isolated copper

was warmed then recooled to 20 K, the overall intensity diminished and the broad continuum split into two portions; the stronger had a maximum at 318.5 nm and the weaker appeared as a shoulder at 310.6 nm. At lower initial concentrations two poorly resolved, broad components were apparent, whose maxima occurred at about 319.0 and 312.5 nm. The interpretation of this spectrum is difficult in the absence of other studies like fluorescence.

C. Gold

1. SF_6

The spectrum of gold-SF_6 solid solutions is relatively simple. Two sharp, strong lines appear at 261.0 nm and 237.8 nm representing blue shifts of 955 and 878 cm^{-1} from the $^2P_{3/2,1/2} \leftarrow {}^2S_{1/2}$ transitions of the free atom respectively. The half-widths of these lines are of the order of 75 cm^{-1} at 20 K and increases as the temperature is raised. Both lines also have their maxima shifted towards lower energies when the temperature is increased. At large gold concentrations, an additional band of small intensity shows up at 298.1 nm. The large spin-orbit splitting of the ^2P term in the free atom apparently remains intact in the SF_6-isolated atom and clearly cannot be responsible for the width of the matrix lines, an idea invoked by Schnepp in his interpretation of the spectrum of matrix-isolated magnesium.

2. Krypton

So efficient is the isolation of gold atoms in a krypton matrix that optically thick films can be grown with a gold temperature of 1420 K and a deposition time of 30 minutes. In a few experiments mercury was

Table IV. Absorption frequencies of matrix-isolated gold at 20 K

Matrix	λ(nm)	ν(cm^{-1})	Assignment	$\nu-\nu_0$(cm^{-1})
SF_6 (M/R = 150)	298.1 ± 0.5	33,546 (w)	?	
	261.0 ± 0.2	38,413 (s)	$^2P_{1/2} \leftarrow {}^2S$	+ 955
	237.8 ± 0.2	42,052 (s)	$^2P_{3/2} \leftarrow {}^2S$	+ 878
Krypton (M/R = 350)	335.6 ± 0.5	29,797 (w)	?	
	271.1 ± 0.5	36,887 (w)	?	
	261.1 ± 0.2	38,300 (s)	$^2P_{1/2} \leftarrow {}^2S$	+ 941
	239.9 ± 0.2	41,684 (sh)	?	
	235.3 ± 0.4	42,499 (s)	$^2P_{3/2} \leftarrow {}^2S$	+1325
	232.5 ± 0.4	43,011 (s)		+1837
Xenon (M/R = 300)	271.3 ± 1.0	36,860 (w)	$^2P_{1/2} \leftarrow {}^2S$	- 499
	247.8 ± 1.0	40,355 (sh)	$^2P_{3/2} \leftarrow {}^2S$	- 819
	244.1 ± 1.0	40,969 (m)		- 205

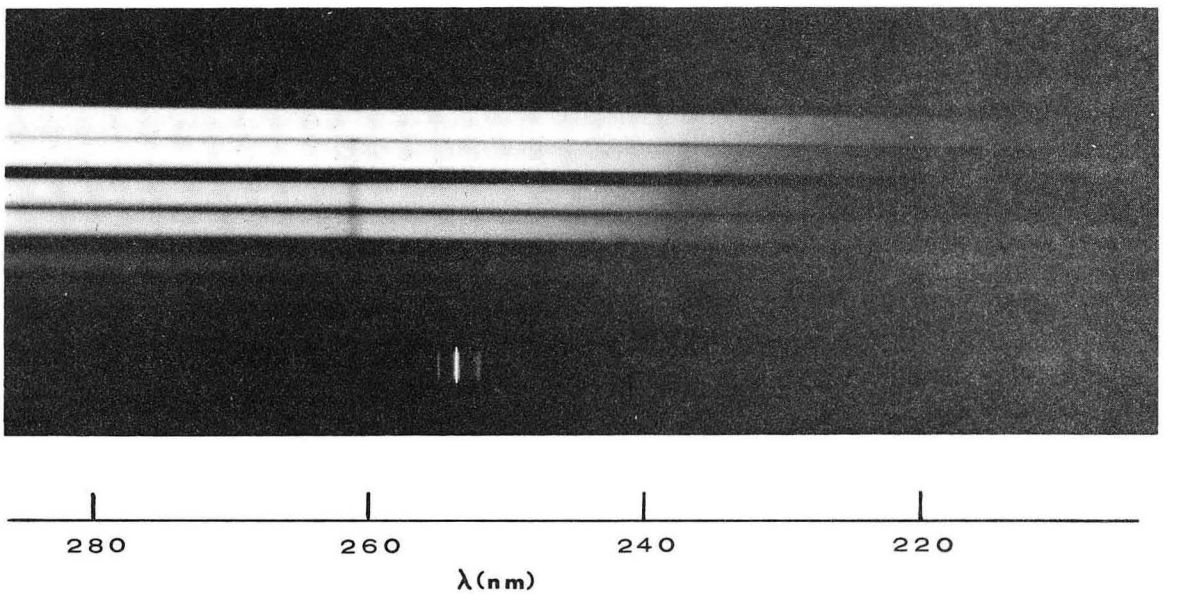

XBB 683-934

Fig. 11. Absorption spectrum of gold atoms isolated in SF_6.

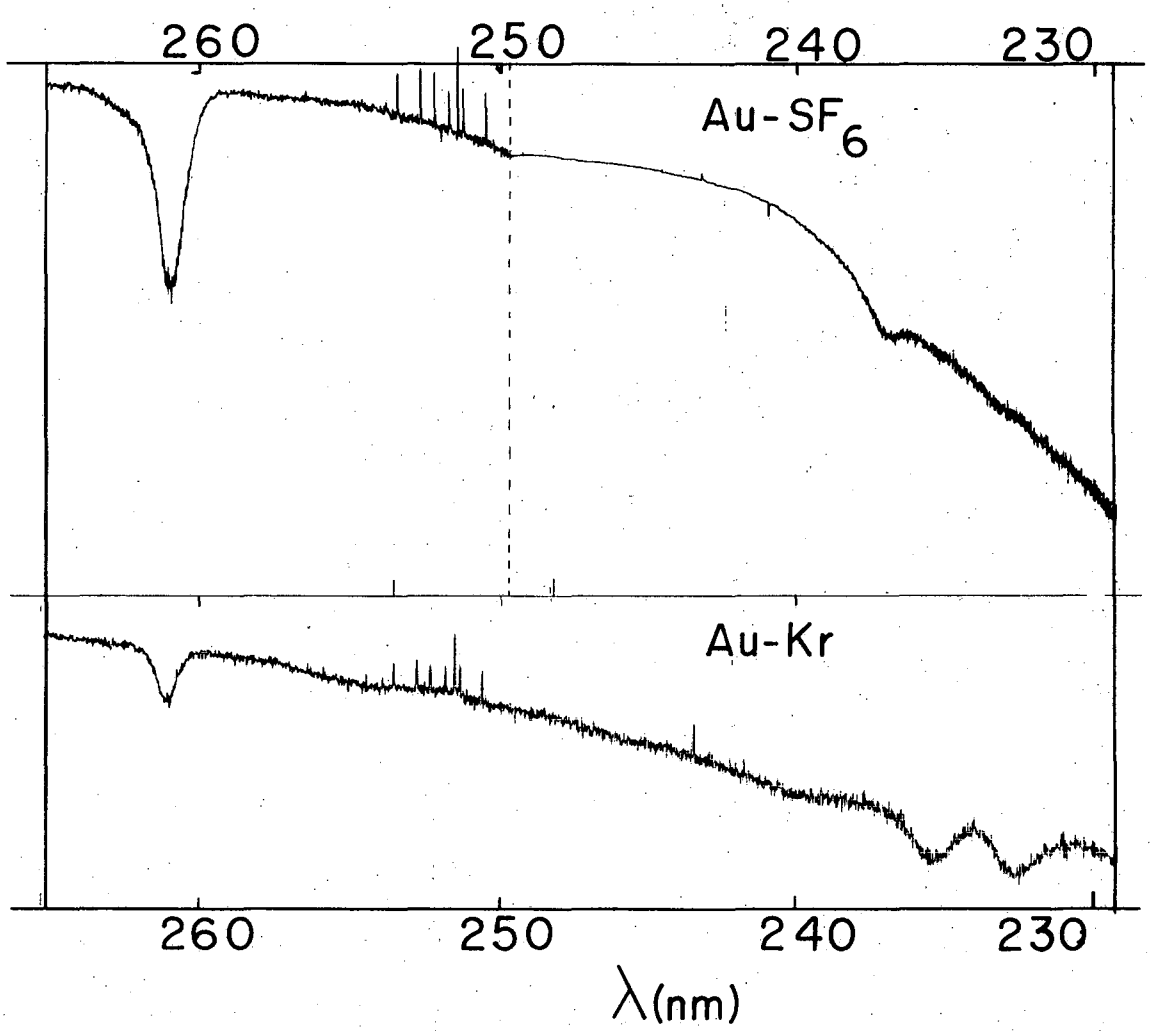

XBL 6810-6043

Fig. 12 Absorption spectra of matrix-isolated gold.

inadvertently present but seemed to have had no effect on the gold band-positions or widths. The spectrum consists of a strong singlet absorption (ν_1) at 261.1 nm and an equally strong doublet (ν_2, ν_3) at 235.3 and 232.5 nm [the values quoted for ν_2, ν_3 (236.0 and 233.3 nm) in an earlier paper (to be published) were in error]. Halfwidths are of the order of 100 cm^{-1} for ν_1 and 250 cm^{-1} for ν_2 and ν_3. At fairly high gold concentrations two additional bands appear - one at λ 239.9 nm as a weak shoulder on the ν_2 band and the other as a weak but fairly narrow line at 271.1 nm.

Correlation of the strong absorptions to the $^2P \leftarrow {}^2S$ transitions of the free atom again show the blue shifts to be large and of the same order of magnitude as those observed for copper and silver trapped in krypton. The weak bands may be due to molecular gold, although these have not been reported for the gaseous dimer.

3. Xenon

Xenon does not appear to isolate gold atoms very well. Relatively high gold temperatures and long deposition times are required to obtain an absorption spectrum of even moderate intensity. Furthermore, the bands are extremely broad with half-widths of the order of 450 cm^{-1}. A single broad band occurs at 271.3 nm which may be correlated to the $^2P_{1/2} \leftarrow {}^2S_{1/2}$ transition of the free atom and a poorly resolved doublet at 247.8 and 2441.1 nm corresponding to the $^2P_{3/2}$ level in the gaseous atom. In contrast to the behavior in SF_6 and Kr, all three bands are shifted to the red with respect to the free atom transitions.

Table V. Absorption frequencies of gold cocondensed with perfluoro-n-heptane at 20 K

λ (nm)	ν (cm^{-1})	Δ (cm^{-1})
268.7 ± 0.2	37,211 (w)	
		366
266.1 ± 0.5	37,577 (w)	
		525
262.4 ± 0.2	38,102 (m)	
		496
259.1 ± 0.2	38,598 (s)	
		481
255.9 ± 0.2	39,079 (s)	
		487
252.7 ± 0.2	39,566 (s)	
		506
249.6 ± 0.2	40,072 (s)	
		496
246.5 ± 0.2	40,568 (vs)	
		491
243.6 ± 0.2	41,059 (s)	
		511
240.6 ± 0.2	41,570 (s)	
		500
237.7 ± 0.2	42,070 (s)	
		489
235.0 ± 0.5	42,559 (w)	
		483
232.3 ± 0.5	43,042 (w)	

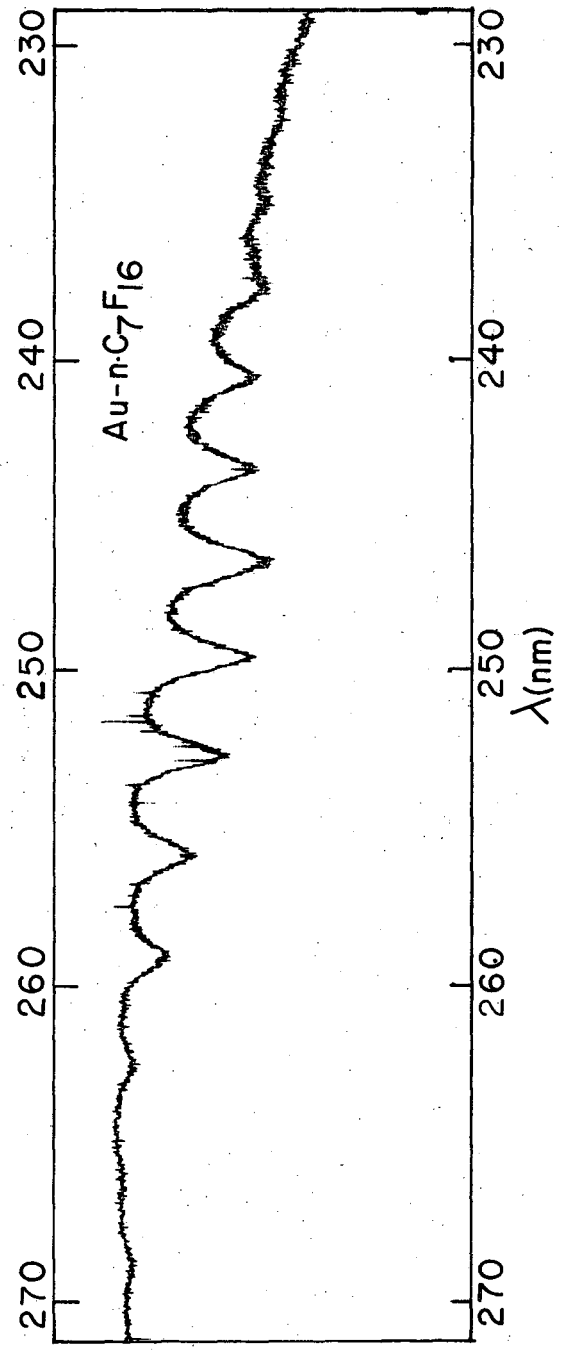

Fig. 13 Absorption spectrum of gold cocondensed with n-perfluoroheptane at 20 K

4. Perfluoro n-Heptane

Gold vapor at 1350 K was cocondensed with the vapor from n-C_7F_{16} liquid contained in a glass tube held at room temperature. The absorption spectrum of the film was surprisingly complex and of a molecular nature as shown in Fig. 13. No attempt was made to elucidate this spectrum.

D. Ag, Au Codeposited in Krypton

The assumption has been made up to this point that all the strong bands observed in the absorption spectra of the noble metals in rare gas matrices are atomic in origin. One may choose to question the validity of this assumption. We may reasonably expect to find at least one transition due to atoms in view of the fact that the vapor in equilibrium with the condensed phase is overwhelmingly monomeric, with the proviso that surface polymerization is negligible. Could the other features then be due to long-range non-nearest neighbor solute-solute interaction? In fact this suggestion has been proffered to explain some features in the spectrum of lithium trapped in krypton.* In order to test out this hypothesis

* Andrews, L. S. and Pimentel, G. C.: J. Chem. Phys. 47, 2905 (1967).

silver and gold were vaporized simultaneously in electron bombardment heated Knudsen cells and codeposited with krypton at 20 K. M/R_{total} ratios of 150, 300 and 500 were used. To obtain comparable intensities, $R_{Ag}/R_{Au} = 2$ was used. The spectra of the pure metals (a,b) and the mixed metal (a',b') in krypton are compared in Fig. 14 and the wavelengths listed in Table VI for $M/R_{total} = 150$. The figure compares the shapes

Table VI. Absorption spectra for silver and gold codeposited in krypton at 20 K

λ (nm)	ν (cm^{-1})	Assignment
322.8 ± 0.5	30,979	Ag
313.8 ± 0.5	31,867	$^2P_{3/2,1/2} \leftarrow {}^2S$
309.5 ± 0.5	32,310	
261.1 ± 0.2	38,300	
239.5 ± 0.2	41,754	Au
235.3 ± 0.4	42,499	$^2P_{3/2,1/2} \leftarrow {}^2S$
232.7 ± 0.4	42,974	

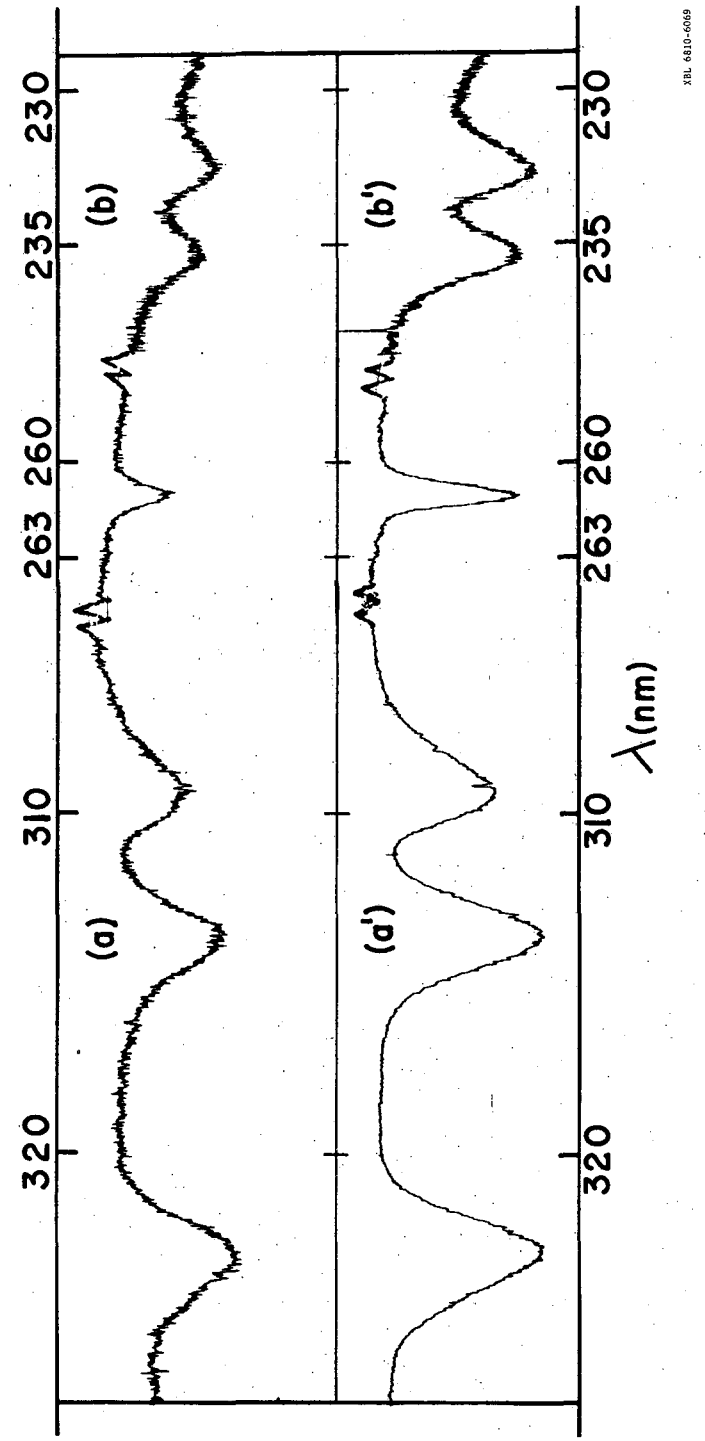

Fig. 14 Absorption spectra of silver and gold isolated in krypton (a,b) separately (a', b') simultaneously.

and positions only of the bands. The relative intensities have no significance since the photographic plates were not previously calibrated and different densitometer settings were used for tracing different sections of the spectrum. It is seen that within experimental error the 'pure' metal bands experience no shift in the presence of the other metal and that no new features appear, at least for the M/R ratios studied. This is conclusive evidence that none of the three strong bands are due to solute-solute interaction. If they were, we should have observed an isotopic-substitution type effect, but much larger, due to Ag Au. Let us examine the statistics of a silver-krypton system in which M/R = 500. For simplicity a metal atom is assumed to be present in a substitutional site having 10 nearest neighbors and 20 next-nearest neighbors. We designate an isolated silver atom as AgKr, a silver atom having another silver atom as nearest-neighbor as Ag Ag, and one having a silver atom as next nearest neighbor as Ag Kr Ag. The ratios of the probability of a solute atom entering these groups is 50:1:2. In other words for 56 atoms arriving in the lattice, 50 will be present as AgKr, 2 as AgAg and 4 as AgKrAg or in terms of percentages 89.5, 3.5 and 7, respectively. Of course similar values are obtained for gold-krypton. If we now co-deposit silver and gold in krypton so that Ag/Au = 1 and $M/R_{total} = 500$, similar arguments suggest that again 89.5% of the total number of atoms will be isolated as Ag Kr and Au Kr in equal amounts, 3.5% will be present as AuAg, AuAu, AgAg pairs, the number of each pair being equal; and 7% as AuKr Au, AuKr Ag, AgKr Ag again evenly distributed. Therefore from the point of view of optical absorption measurements, if the f-values for the transitions involving the three species AuAu, AuAg, AgAg are comparable, any effects due to nearest neighbor or next-nearest neighbor solute-solute

interaction in the pure metal experiments and which are still present in the mixed metal circumstance should be large enough to be manifested as AgAu interactions. The fact that these effects were not observed for Ag/Au = 2, 1, 1/2 and M/R = 150, 500 demonstrates that none of the three main bands in the pure metal matrix spectrum are due to solute-solute interaction. It appears then that under the conditions investigated, each trapped solute atom in the pure or mixed situation is efficiently shielded from the effects of other solute atoms by the atoms of rare gas in both the first and second coordination shells.

It may be noted also that the concentrations of atoms in the mixed metal experiments were such that the weak bands of the pure metal spectra were not in evidence. As a result it was not possible to apply the above argument to determine whether these weak bands were due to dimer. However further experiments in which these bands would be the point of emphasis should be instructive. The electronic spectra investigation should be supplemented by infrared methods of detection of the asymmetric diatomics.

E. Copper-Gold Alloy in Krypton

The trapping of the vapor species from an Au-Cu alloy was intended to study further the possibility of solute-solute interaction in the matrix. An alloy having a mole fraction of copper (X_{Cu}) of 0.28 was selected in order to obtain comparable vapor pressures ($P = 4 \times 10^{-5}$ torr) of copper and gold at 1350 K. The results of such an experiment using krypton as the matrix material are shown in Table VII. Actually mercury atoms were also present as a contaminant. The gold absorptions were much more intense and narrower than those of copper, as was the case for the pure metals. More importantly there were no shifts of the bands from the positions in the pure metals and no appearance of new bands, again

justifying the conclusion that the three prominent bands in the spectrum of each metal are due to atoms. The absence of any Au-Cu interaction is possibly due to a concentration effect - not enough diatomic molecules are present to be seen in absorption. The same recommendations are made here as for the Ag-Au/Kr system.

F. Gold in SF_6 - Kr Mixtures

The large shifts and multiplet structures seen in the absorption spectra of trapped noble-metal atoms seem to indicate that the matrix environment possesses a certain degree of asymmetry. In an effort to examine more closely this effect of the asymmetry of the environment on the absorption spectra of the atoms, gold was trapped at 20 K in various mixtures of krypton and sulfur hexafluoride. The mixtures were equilibrated for at least 18 hours; gold temperatures of 1350-1375 K were used and the M/R ratios varied between 700 and 400. The results of these experiments are summarized in Table VIII and representative spectra are shown in Fig. 15.

A noticeable difference lies in the width of the lines. The long wavelength component ν_1 which was so narrow in the pure matrices has its half-width almost doubled. In addition the position of its maximum seems to be dependent on the composition of the matrix mixture, being shifted if at all, to lower energies with respect to either pure SF_6 or pure Kr. The central band ν_2 also has an increased half-width and the largest shift of its maximum is only 1 nm to the red of ν_2 in pure SF_6. With respect to ν_2 for pure Kr, ν_2 for all the mixtures are shifted to the red by a fair amount. The short wavelength component ν_3 which has no counterpart in pure SF_6 is much broader than ν_3 for pure Kr. The position of its maximum is difficult to locate precisely because of its

Table VIII. Absorption frequencies of gold isolated in Kr-SF_6 mixtures at 20 K

Mole-% Kr	λ (nm)	ν (cm^{-1})	Δ(cm^{-1}) cf. SF_6	Δ(cm^{-1}) cf. Kr
7	261.1	38,298	-16	0
(M/R = 700)	237.7	42,070	+18	-429
	233.7	42,790		-221
17	261.1	38,298	-16	0
(M/R = 450)	237.2	42,160	+108	-339
	232.8	42,952		- 59
50	262.5	38,095	-219	-203
(M/R = 600)	238.2	41,982	- 70	-517
	230.8±0.5	43,328		+317
75	262.8	38,052	-262	-246
(M/R = 350)	238.8	41,876	-176	-623
	230.5	43,384		+373
83	262.8	38,052	-262	-246
(M/R = 400)	238.5	41,929	-123	-570
	231.0	43,290		+180

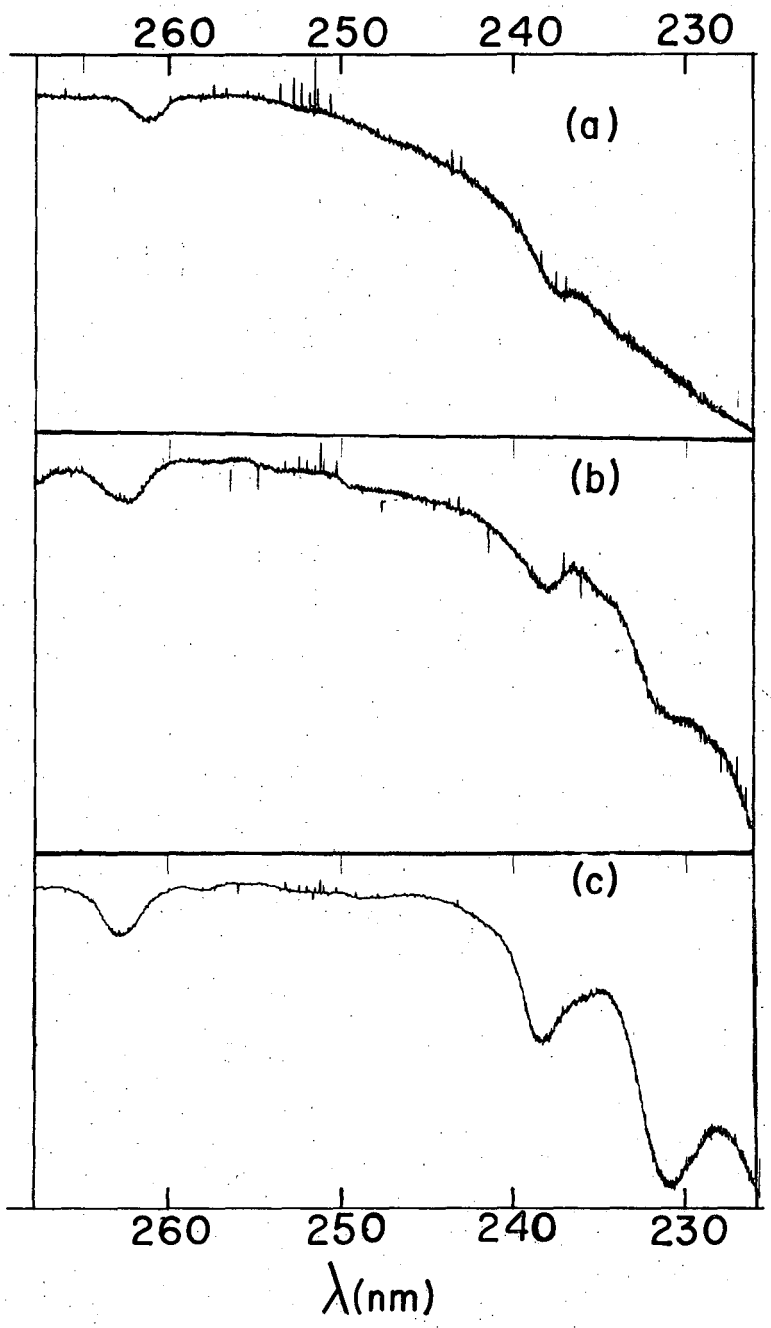

XBL 6810-6045

Fig. 15 Absorption spectra of gold trapped in solid SF_6-Kr mixtures (a) 17 mole-% Kr, (b) 50 mole-% Kr, (c) 83 mole-% Kr

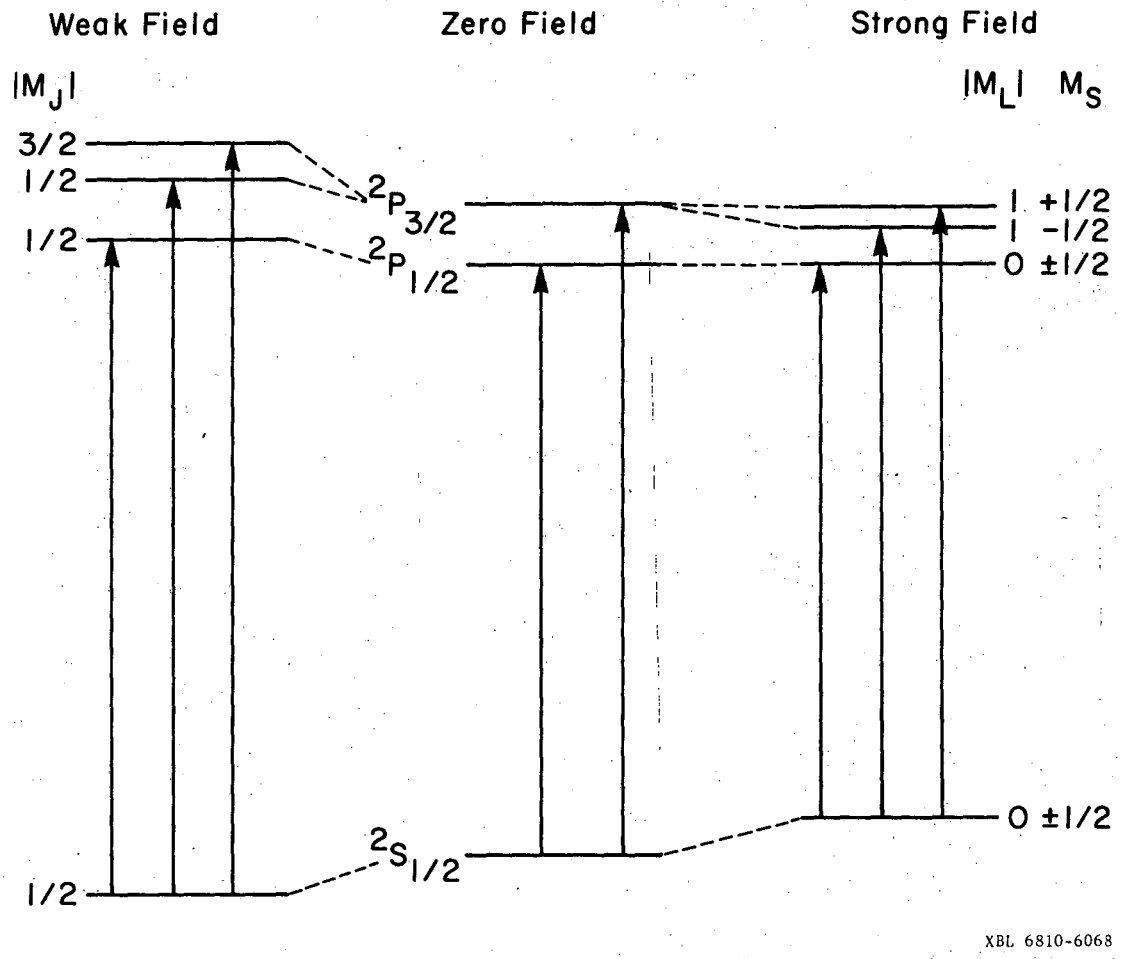

Fig. 16 Stark effect on ^2P terms

relatively low intensity even when photographed on SWR plates. However it shows a rather erratic behavior, being red-shifted at some compositions and blue-shifted for compositions larger than 50 mole-percent of Kr.

In the light of our previous correlation of ν_2 and ν_3 with the $^2P_{3/2}$ state of the free atom, it is seen that the doublet separation $(\nu_3 - \nu_2)$, while not showing a clear trend, seems to depend on the type of environment in which the atom is embedded. This brief study in SF_6-Kr mixtures is insufficient to enable us to assess the details of this environment in terms of symmetry. It is questionable that the atoms are located in sites which experience an average behavior of Kr and SF_6 nearest neighbors. Rather there seems to be a segregation of predominantly SF_6 and predominantly Kr sites in the solid mixtures, the composite spectrum then being akin to a near-superposition of perturbed SF_6 and perturbed Kr spectra.

V. CONCLUDING REMARKS

This work can only be regarded as a small effort towards improving our understanding of the behavior of atoms embedded in a low temperature matrix. It has been shown that

(a) the matrix-isolated atoms of the noble metals show shifts from the free atom transitions which increase from xenon to krypton to argon. This is in conformity with the general trend observed for a number of other atoms.

(b) Non-nearest neighbor solute-solute interactions do not account for any of the major absorptions in the spectra of copper, silver and gold which are already predominantly monomeric in the vapor phase.

We are led to the conclusion that the matrix molecular presence is solely responsible for the multiplet structure of these atomic spectra. It is still not clear by what mechanism this is accomplished. The transitions studied in the noble metal atoms again involve excited P states, which has almost always been the case for the atoms previously studied. The theory that the observed triplet structure may be due to the removal of the three-fold degeneracy of the excited P state by an asymmetric environment remains a plausible one. It must be borne in mind however that interatomic electric fields can be quite large and probably capable of producing a Stark-like effect on the atomic terms. Figure 16 illustrates the Stark effect on ^2P terms. It is seen that irrespective of the strength of the field, three sub-states result from the lifting of some J-degeneracies. It may be very instructive to pursue the study of the role of these long-range electrostatic interactions by isolating atoms in chemically inert matrices with permanent dipole

moments. A start has been made in this direction by looking beyond the rare gases to inert fluorinated compounds like sulfur hexafluoride and n-perfluoroheptane whose use has been reported in this study. These preliminary results however give a preview of the sort of difficulties that may be encountered in the use of so-called chemically inert materials.

ACKNOWLEDGEMENTS

I wish to express my profound and sincere appreciation to Professor Leo Brewer not only for his inspiring technical direction but also for the sense of camaraderie which his own personality is able to engender in every member of his research group.

Dr. David Meschi gave me the benefit of his considerable experience during the design and construction of the electron bombardment-heated furnace and for this I am very grateful. My thanks also to Professor John Newman for his help in the problems of heat transfer.

This work was performed under the auspices of the United States Atomic Energy Commission.

APPENDIX

Estimation of Radiant Heat Flux and Temperature Gradients at Target

Let us consider the radiant heat transfer between two black surfaces 1 (graphite cell) and 2 (sapphire plate). If θ is the angle measured from the normal to the surface, then the energy q_θ emitted per unit area per unit time per unit solid angle in a direction θ is given by Lambert's law

$$q_\theta = \frac{\sigma T_1^4}{\pi} \cos \theta$$

The radiant energy emitted by A_1 and intercepted by dA_2 per unit time is then

$$q_{12} = \frac{\sigma T_1^4 A_1}{\pi} \cos \theta \cdot \cos \theta \frac{dA_2}{r^2}$$

where r is the distance between the two surface elements and $r^2 = x^2 + y^2 + z^2$.

If z_0 is the perpendicular distance between the two surfaces and x, y define the sapphire surface then $\cos \theta = z_0/r$ and the radiant energy transferred to unit area of sapphire plate per unit time is

$$q_{12} = \left(\frac{\sigma T_1^4 A_1}{\pi r^2}\right)\left(\frac{z_0^2}{r^2}\right) = \frac{\sigma T_1^4 A_1 z_0^2}{\pi(r^2 + y^2 + z^2)^2}$$

This equation shows that the radiant flux is a maximum at the center of the plate (x,y = 0,0) and equal to

$$q_{max} = \frac{\sigma T_1^4 A_1}{\pi z_0^2}$$

In our system z_0 = 50 mm, A_1 = 75 mm^2 and

$$q_{max} = \frac{(1.355 \times 10^{-14})(1.336 \times 10^3)^4 (75)}{(3.142)(50^2)}$$

or $q_{max} = 4.0 \times 10^{-4}$ cal sec^{-1} mm^{-2}.

We can now estimate the temperature gradient across the thickness or length of the plate with the assumption that all the radiation impinging on the surface is absorbed by the plate and that steady state heat conduction obtains. Integration of Fourier's law of heat conduction

$$q_z = - k \frac{\partial T}{\partial z}$$

gives for constant q_z and k

$$q \cdot z = -k\, T_z + c$$

in which c is the integration constant. If $T = T_0$ at $z = 0$, q is negative and $c = kT_0$ then

$$(T-T_0) = - \frac{qz}{k} \quad .$$

LEGAL NOTICE

TECHNICAL INFORMATION DIVISION
LAWRENCE RADIATION LABORATORY
UNIVERSITY OF CALIFORNIA
BERKELEY, CALIFORNIA 94720